Title

The functional architecture for face-processing expertise: FMRI evidence of the developmental trajectory of the core and the extended face systems

Journal

Neuropsychologia, 51(13)

ISSN

00283932

Authors

Haist, Frank
Adamo, Maha
Han Wazny, Jarnet
et al.

Publication Date

2013-11-01

DOI

10.1016/j.neuropsychologia.2013.08.005

Peer reviewed

Published in final edited form as:
Neuropsychologia. 2013 November ; 51(13): . doi:10.1016/j.neuropsychologia.2013.08.005.

The Functional Architecture for Face-processing Expertise: FMRI Evidence of the Developmental Trajectory of the Core and the Extended Face Systems

Frank Haist[a,b,*], **Maha Adamo**[b], **Jarnet Han**[b], **Kang Lee**[c], and **Joan Stiles**[b,d]

[a]Psychiatry Department, University of California, San Diego, 9500 Gilman Drive, La Jolla, CA 92093-0115 USA

[b]Center for Human Development, University of California, San Diego, 9500 Gilman Drive, La Jolla, CA 92093-0115 USA

[c]Dr. Eric Jackman Institute of Child Study, University of Toronto, 45 Walmer Road, Toronto, Ontario M5R 2X2 Canada

[d]Cognitive Science Department, University of California, San Diego, 9500 Gilman Drive, La Jolla, CA 92093-0115 USA

Abstract

Expertise in processing faces is a cornerstone of human social interaction. However, the developmental course of many key brain regions supporting face preferential processing in the human brain remains undefined. Here, we present findings from an FMRI study using a simple viewing paradigm of faces and objects in a continuous age sample covering the age range from 6 years through adulthood. These findings are the first to use such a sample paired with whole-brain FMRI analyses to investigate development within the core and extended face networks across the developmental spectrum from middle childhood to adulthood. We found evidence, albeit modest, for a developmental trend in the volume of the right fusiform face area (rFFA) but no developmental change in the intensity of activation. From a spatial perspective, the middle portion of the right fusiform gyrus most commonly found in adult studies of face processing was increasingly likely to be included in the FFA as age increased to adulthood. Outside of the FFA, the most striking finding was that children hyperactivated nearly every aspect of the extended face system relative to adults, including the amygdala, anterior temporal pole, insula, inferior frontal gyrus, anterior cingulate gyrus, and parietal cortex. Overall, the findings suggest that development is best characterized by increasing modulation of face-sensitive regions throughout the brain to engage only those systems necessary for task requirements.

Keywords

Functional MRI; Brain Development; Fusiform Face Area: Face Processing Expertise; Core and Extended Face Networks

*Corresponding author. Tel.: +1-858-822-5456; fax: +1-858-822-1602.

1. Introduction

Human beings are social animals by nature (Aristotle, 350 B.C.E.; Spinoza, 1677). That fact explains the increasing interest in the field of social neuroscience aimed at discovering the neural architecture supporting human social behavior. Faces are arguably the most important visual stimuli in our social environment. As the fulcrum of our social interaction with others, it is not surprising that adults are expert face processors. Adult expertise is characterized by the near universal ability to rapidly and accurately discriminate individuals from amongst thousands of highly similar faces encountered routinely and to extract extensive information about individuals from brief exposures to face stimuli.

Advances in functional neuroimaging are largely responsible for the significant increase in our understanding of the mature brain architecture for human face processing in typical and atypical populations (Avidan & Behrmann, 2009; Behrmann & Avidan, 2005; Haxby, Hoffman, & Gobbini, 2002; Kanwisher & Yovel, 2006; Tsao & Livingstone, 2008). Brain regions within the “core” face system process the invariant aspects of faces, such as facial features and identity (Haxby, Hoffman, & Gobbini, 2000). The core regions include the functionally defined fusiform face area (FFA) in the middle fusiform gyrus (see Kanwisher & Yovel, 2006), the occipital face area (OFA) in the lateral inferior occipital gyrus (see Gauthier, et al., 2000; Rossion, et al., 2003), and the posterior superior temporal sulcus (pSTS) (Haxby, et al., 2000). Recent studies suggest that the fusiform gyrus may include multiple distinct face preferential processing regions occupying the posterior and anterior aspects of the middle fusiform gyrus (Pinsk, et al., 2009; Weiner & Grill-Spector, 2012). We use the acronym FFA to infer all regions (i.e., voxels) within the fusiform gyrus that show a functionally defined preference to faces (e.g., face activity > activity to diverse objects). This approach closely aligns the present study with previous studies of development of the core face network regions. One important feature of the mature core system, particularly the FFA and OFA, is that these regions are activated when viewing faces largely regardless of specific task demands. That is, activation is observed whether the task requires active face processing, such as remembering or matching specific faces (Epstein, Higgins, Parker, Aguirre, & Cooperman, 2006; Gauthier, Curby, Skudlarski, & Epstein, 2005; Mazard, Schiltz, & Rossion, 2006; Xu, 2005; Yovel & Kanwisher, 2004, 2005), passive viewing (Grill-Spector, Knouf, & Kanwisher, 2004; Haist, Lee, & Stiles, 2010; Kanwisher, McDermott, & Chun, 1997; Kanwisher, Stanley, & Harris, 1999; Rhodes, Byatt, Michie, & Puce, 2004; Wojciulik, Kanwisher, & Driver, 1998), or implicit presentation (Cantlon, Pinel, Dehaene, & Pelphrey, 2011; Kouider, Eger, Dolan, & Henson, 2009; Morris, Pelphrey, & McCarthy, 2007). Activation of the pSTS is most closely associated with dynamic feature processing, such as monitoring eye gaze and mouth movements, and is thus observed in tasks in which these actions are factors (Ishai, Schmidt, & Boesiger, 2005; Rolls, 2007).

In contrast, the recruitment of brain areas within the mature “extended” face system tends to be task-specific (Fairhall & Ishai, 2007; Gobbini & Haxby, 2007; Haxby, et al., 2001; Haxby, et al., 2000; Ishai, et al., 2005). For example, activation of the amygdala, insula, and other limbic system areas occur when tasks require the analysis of the emotional content of faces (Bzdok, et al., 2011; Gobbini & Haxby, 2007; Ishai, Pessoa, Bikle, & Ungerleider, 2004; Schulz, et al., 2009). Recollection of semantic knowledge for faces may engage the inferior frontal gyrus, whereas episodic memory retrieval may recruit the precuneus, posterior cingulate cortex, and medial temporal lobe (Brambati, Benoit, Monetta, Belleville, & Joubert, 2010; Gobbini & Haxby, 2007; Leveroni, et al., 2000). Analysis of intentions can activate the region of the temporal-parietal junction, whereas processing attitudes and mental states recruits the anterior cingulate cortex (Kaplan, Freedman, & Iacoboni, 2007; Redcay, et al., 2010). Regions of the anterior temporal pole may be active in tasks requiring individuation of faces and biographical information retrieval (Gobbini & Haxby, 2007;

Kriegeskorte, Formisano, Sorger, & Goebel, 2007; Nestor, Plaut, & Behrmann, 2011; Nestor, Vettel, & Tarr, 2008). In summary, recruitment of the regions included in the extended network presumably reflects the fact that many face tasks require processing of a wide array of information beyond the general appearance of the face.

In contrast to the adult literature, the body of evidence regarding the brain architecture of face processing in childhood is limited. Behavioral data show that the ability to process faces as distinctive visual stimuli begins in the first year of life. Newborns show a preference for and can discriminate faces from other classes of objects and abstract stimuli (Bushnell, Sai, & Mullin, 1989; Cassia, Turati, & Simion, 2004; Johnson & Morton, 1991; Turati, Simion, Milani, & Umiltà, 2002). By 3 months, infants can categorize faces by gender, race, and attractiveness (Kelly, et al., 2007; Kelly, et al., 2005; Langlois, Ritter, Roggman, & Vaughn, 1991; Quinn, Yahr, Kuhn, Slater, & Pascalis, 2002; Slater, et al., 2000a; Slater, Quinn, Hayes, & Brown, 2000b), and by 5 to 7 months they begin to rely on both featural and configural information for face identification (Cohen & Cashon, 2001). Despite these early abilities, the behavioral evidence is strong that expertise in face processing develops slowly and over many years (for review see Lee, Quinn, Pascalis, & Slater, 2013). For example, children have difficulty processing featural and configural information relevant to face identification through the school-age period (Mondloch, Le Grand, & Maurer, 2002). The pattern of children's featural processing reaches adult levels at about 10 to 11 years, before which they first rely on outer face features for face identification and then gradually shift to rely on inner face features (Want, Pascalis, Coleman, & Blades, 2003). Extraneous features such as clothing and hairstyle easily distract children under 10 to 11 years when identifying individual faces (Freire & Lee, 2001; Mondloch, et al., 2002). In summary, the behavior literature suggests that face-processing expertise shows an extended developmental trajectory reaching into adolescence.

The emerging cognitive neuroscience literature is consistent with the behavioral evidence for the protracted development of face-processing expertise. Most of the neural imaging work using event-related potential (ERP) methodologies has revealed an early onset of neural markers specific for faces. For example, the N170, a negative deflection with peak latency of approximately 170 msec, is consistently observed in studies of face processing (for review see Lee, et al., 2013). However, despite their early onset, these markers undergo gradual development to reach the adult level only in adolescence (de Haan, Pascalis, & Johnson, 2002; Taylor, Batty, & Itier, 2004). In contrast to ERP methodologies that have exquisite temporal resolution but very poor spatial resolution, researchers have mainly relied on FMRI methodologies to study the cortical regions involved in the development of face processing expertise. Some FMRI studies have focused on development within the ventral posterior regions generally with findings showing a pattern of increasing specification in the location of face-selective regions (Aylward, et al., 2005; Gathers, Bhatt, Corbly, Farley, & Joseph, 2004; Passarotti, et al., 2003). One early study reported a shift from more diffuse to more focal activation within the ventral occipito-temporal cortex (VOT) (Passarotti, et al., 2003). Subsequent studies suggest that the basic pattern of developmental change involves a shift in the locus of activation from divergent areas within the VOT to the fusiform gyrus (Aylward, et al., 2005; Gathers, et al., 2004; Golarai, Liberman, Yoon, & Grill-Spector, 2010; Scherf, Behrmann, Humphreys, & Luna, 2007). Many studies have focused on the FFA and OFA components of the core face network specifically; yet, there remains considerable controversy about the developmental trajectory of the FFA. Some studies of young school age children failed to find activation within the regions that are typically associated with the mature FFA, while others have reported adult-like FFA activation intensity in children. For example, two studies that included children as young as 4 years suggested the FFA reaches mature levels of activity and extent of fusiform gyrus (FG) activation by 7 years (Cantlon, et al., 2011; Pelphrey, Lopez, & Morris, 2009). Nevertheless,

the preponderance of evidence suggests significant developmental change within the FFA well beyond this time extending through mid to late adolescence. Gathers et al. (2004) reported that younger children (5–8 years) did not show reliably greater activation for faces relative to objects within the FFA, whereas older children (9–11 years) showed reliable face selectivity within the FFA. Similarly, Scherf and colleagues (2007) reported that children 5 to 8 years do not activate the classic FFA, but instead tend to produce face-preferential activation in the posterior ventral processing system putatively involved in featural processing. Several groups have reported that development of face preferential activation in the fusiform gyrus is associated with systematic increases in the size (Brambati, et al., 2010; Cohen Kadosh, Johnson, Dick, Cohen Kadosh, & Blakemore, 2012; Golarai, et al., 2007; Peelen, Glaser, Vuilleumier, & Eliez, 2009; Scherf, et al., 2007) and intensity of activation (Brambati, et al., 2010; Cohen Kadosh, Cohen Kadosh, Dick, & Johnson, 2011; Golarai, et al., 2007; Joseph, Gathers, & Bhatt, 2011). Developmental changes in face preferential activation in fusiform gyrus volume and intensity have also been found using FMRI adaptation paradigms (Cohen Kadosh, Henson, Cohen Kadosh, Johnson, & Dick, 2010; Scherf, Luna, Avidan, & Behrmann, 2011). Further, increases in FFA volume and activation intensity correlate with improvement in recognition memory for faces (Golarai, et al., 2007; Golarai, et al., 2010). This underscores an issue that may cloud clear interpretations of the development of face-processing abilities; specifically, many developmental studies evaluate face processing within the context of memory tasks, such as the sparse one-back localizer memory task, or some other active judgment task (Golarai, et al., 2007; Golarai, et al., 2010; Passarotti, et al., 2003; Passarotti, Smith, DeLano, & Huang, 2007; Peelen, et al., 2009; Pelphrey, et al., 2009). This led Scherf and colleagues (2011) to suggest that task demands may influence some of the developmental differences observed in fusiform gyrus.

The prolonged developmental path to reach mature face processing is supported from the analysis of functional connectivity as well. Cohen Kadosh and colleagues (2011) evaluated effective connectivity (i.e., directional functional connectivity) of face-related VOT regions using Dynamic Causal Modeling (Fairhall & Ishai, 2007; Friston, Harrison, & Penny, 2003). They scanned younger (7–8 years) and older (10–12 years) children and adults during face identity, emotion, and gaze detection tasks and found that all groups produced the same basic network structure that included a region of the inferior occipital gyrus (IOG) that influenced activation in the FG and the superior temporal sulcus (STS). This suggested that the basic VOT face network is observed in children as young as 7 years. However, the magnitude of effects among the child groups differed from adults. The old and young child groups exhibited weaker connectivity between IOG and FG, and no significant connectivity between IOG and STS. Furthermore, the effects of task demand differentiated the adults and children. Different tasks selectively modulated network patterns in adults; specifically, the identity task increased IOG influence on FG, whereas the expression task increased IOG influence on STS. Children did not show such selective task effects.

The focus of developmental face studies is expanding to appraise face-related activity outside the ventral occipitotemporal regions to include whole brain-analysis including regions of the extended face network. Note that although some imaging studies that focused on the core system regions reported results from whole-brain analyses, these data were typically not the central focus of investigation and the active areas were used largely to guide region of interest (ROI) analyses (c.f., Aylward, et al., 2005; Peelen, et al., 2009). A central question regarding development of the extended face network is whether children show the mature pattern of activation of extended network regions according to task demand, or whether this mature pattern is acquired gradually through development. Studying the status of extended face network activation when there is little to no demands on face processing other than simple viewing of faces can provide important data to address this question. Joseph and colleagues (2011) suggests that extended network activity in

childhood may not be driven by task demands per se. They studied children 5 to 12 years and adults in a simple face and object viewing task that required pressing a button each time the participant was shown a stimulus. They found that children produced significantly greater activation in extended face network regions in the parietal cortex and lateral temporal cortex, but more globally, they noted that children produced greater activation than adults in widespread left hemisphere brain areas in the frontal, temporal, and parietal lobes. These regressive changes with age suggest that increased face expertise might lead to greater selectivity in recruiting brain regions when engaged in face-processing tasks.

Despite significant gains in our understanding of the developmental progression of the neural basis of face expertise, fundamental questions remain unresolved. No single FMRI study has attempted to characterize development of the FFA within the context of whole-brain imaging to evaluate core and extended face regions within a continuous age sample spanning middle childhood, adolescence, and adults. The present study examined the typical neural development of face processing under task conditions that were minimally confounded by extraneous cognitive demands. During FMRI scanning, children, adolescents, and adults viewed pictures of faces, diverse objects, wristwatches, and scrambled stimuli. Instead of requiring them to judge the visual objects specifically, we asked participants simply to detect whether the background color upon which the stimulus was shown had changed. Thus, task demands not only were minimal but also did not explicitly call for face processing. In addition, unlike most prior studies, all stimuli were matched in terms of spectral power, contrast, and brightness to control for possible undue influences of non-critical physical characteristics on face processing. We analyzed brain activation across development in the fusiform gyrus using traditional methods for defining the FFA, including analysis of the volume of activation, activation intensity (percent signal), and the location of the FFA. In addition, we analyzed whole-brain activation to provide a comprehensive review for the role of the extended face network in development during the passive viewing of faces.

The validity of functional MRI studies across groups relies on the assumption that baseline BOLD activity is reasonably equivalent in these groups (Buckner, Andrews-Hanna, & Schacter, 2008). This assumption is rarely considered in developmental studies and has not been addressed in any prior study of face processing. Here, we introduce the application of a new method for BOLD FMRI data preprocessing that controls for estimated physiological artifacts and, more importantly, for individual differences in task-negative activation during face processing. Task-negative activation in adults is spatially coincident to activation in the default mode network (DMN) and developmental differences in the DMN are well established (Fair, et al., 2008; for recent methodological considerations, see Power, Barnes, Snyder, Schlaggar, & Petersen, 2012; Stevens, Pearlson, & Calhoun, 2009; Supekar, et al., 2010; Van Dijk, Sabuncu, & Buckner, 2012). The interpretation of DMN maturation, namely greater integration of the DMN nodes, is hypothesized to support cognitive information integration and strategic organization (Fair, et al., 2008). Thus, developmental differences in task-negative activation may mask or alter the genuine task-positive BOLD activation. The combination of optimized methodological and analytical approaches allows us to evaluate neurodevelopmental differences in face processing with advanced clarity.

2. Materials and methods

2.1 Participants

We tested 90 participants in the experiment, including 43 children age 6–12 years, 23 adolescents age 13–16 years, and 24 adults age 18–37 years. Nineteen participants were subsequently excluded from the study due to excessive motion during FMRI scanning or uncorrectable FMRI artifact, including 13 children (30%), 3 adolescents (13%), and 3 adults

(12%). See Section 2.5.2 for description of inclusionary criteria based on movement and artifact. Thus, the final participant sample was comprised of 71 participants that included 30 children (15 females; mean age [years-months] = 10−8), 20 adolescents (11 females; mean age = 15−9), and 21 adults (9 females; mean age = 25 years). Additional demographic information is provided in Table 1. All participants had normal or corrected-to-normal vision and no history of psychiatric or neurological disease, significant head trauma, or other condition that may negatively impact brain function. In addition, overall cognitive abilities of all participants were estimated at Average or better as measured by scores on a standardized IQ test (Full Scale IQ score ≥ 90). Participants were recruited from the general San Diego region through advertisements or were affiliated with the university. The Human Research Protections Program of the University of California, San Diego approved this study. Participants provided informed consent prior to the study and were paid or given course credit for participation.

2.2 Stimuli

The task used a total of 672 unique gray scale images including 168 male and female faces with neutral expressions, 168 images of diverse objects, 168 images of digital and analog wristwatches, and 168 scrambled stimuli (see Figure 1). The stimuli were obtained from digital pictures and digitized photographs. Scrambled stimuli were created by randomly arranging 3 × 4 pixel segments from images of face, object, and watch stimuli used in the study with the Scramble Photoshop plugin[1], which were then blurred with a 1.2 pixel Gaussian filter. All images were balanced for spectral power, contrast, and brightness to equate lower-level perceptual information (Willenbockel, et al., 2010)[2]. Face stimuli (half male and half female) were obtained from several face databases including the Center for Vital Longevity Face Database (Minear & Park, 2004)[3], Facial Recognition Technology (FERET) database (Phillips, Moon, Rizvi, & Rauss, 2000; Phillips, Wechsler, Huang, & Rauss, 1998)[4], Psychological Image Collection at Stirling (PICS)[5], and from our own database. Face images were isolated within an oval mask. Watch stimuli (half analog and half digital) were obtained from various sources on the Internet with all watches set to the same time (i.e., 10:09). Diverse object stimuli were comprised of stimuli selected from 40 different basic-level categories (e.g., baskets, apples, balls, whistles, vases, cameras, umbrellas, jackets, books, lamps, etc.) that were obtained from various sources on the Internet (i.e., retail sites such as amazon.com) or photographed in the lab. Two versions of each stimulus image were created, one with a white background and one with a gray background. All images were approximately the same size and subtended a horizontal visual angle of approximately 8.5° and a vertical angle of approximately 11.2°.

2.3 Design and procedure

2.3.1 Behavioral testing and training—All participants were administered the Wechsler Abbreviated Scale of Intelligence (WASI; Wechsler, 1999) to obtain scores for Verbal IQ (VIQ), Performance IQ (PIQ), and Full-Scale IQ (FSIQ). A minimum FSIQ score of 85 was required for participation in the study. Children under 9 years were given practice in a simulated MR scanner (i.e., “mock scanner”) that provided training in motion compliance and task requirements before their FMRI test session. All participants received training and practice in the task immediately before their FMRI test session using a separate set of unique stimuli.

[1] http://www.telegraphics.com.au/sw/#scramble
[2] http://www.mapageweb.umontreal.ca/gosselif/shine/
[3] http://agingmind.cns.uiuc.edu/facedb/
[4] http://face.nist.gov/colorferet/
[5] http://pics.psych.stir.ac.uk/

2.3.2 Simple Picture-Viewing Localizer task—A blocked FMRI design was used to present images of intermixed male and female faces, diverse objects, intermixed analog and digital watches, and scrambled stimuli. The watch and scrambled stimuli were presented for use in a separate study and were not used in this study to determine face preferential processing areas. All images were unique; that is, no image was repeated across the task. All stimuli were back-projected onto a screen located at the foot of the scanner bed from an LCD projector located in the scanner control room. Participants viewed the stimuli via a mirror attached the scanner coil above their eyes. Each participant was presented four task runs using unique stimuli in each run (see Fig. 1). Each run included three 14 sec stimulus blocks for each stimulus category (12 stimulus blocks total per run), interleaved with 14 sec fixation epochs (crosshair stimulus only), with an additional 8 sec fixation block at the beginning of each task run. Within each stimulus block, 14 unique images were presented; 10 images were presented on a white background and four images on a gray background (RGB values = 172). Stimuli were presented for 500 msec followed by a 500 msec fixation interval. Participants were instructed to view the pictures and to press a button each time a picture had a gray background. In this fashion, task performance did not require specific analysis of the pictured stimulus per se, but compliance would ensure that participants' attention was engaged. In order to orient participants to the onset of stimulus blocks, the fixation cross that was presented during the fixation period changed from a black standard typeface cross to red bold typeface cross 2 sec prior to the beginning of the stimulus presentation. Each simple picture-viewing localizer run lasted 5 min 44 sec, during which 172 FMRI volumes were obtained (TR=2000 msec). The reaction times for correct responses and response accuracy as defined by d' were calculated for each participant.

2.4 Image Acquisition

Imaging data were obtained at the University of California, San Diego Center for Functional Magnetic Resonance Imaging using a short-bore 3.0 Tesla General Electric Signa EXCITE MR scanner (Waubesha, WI, USA) equipped with a parallel-imaging capable GE 8-channel head coil. FMRI data were acquired using a single-shot gradient-recalled echo-planar imaging sequence with blood oxygenation level-dependent (BOLD) contrast (32 axial slices; 4-mm slab; TR=2000; TE=30 msec; flip angle=90°; FOV=256 mm; matrix=64×64; in-plane resolution=4 mm^2). We used 4 mm isometric voxels rather than higher-resolution voxels to maximize signal-to-noise within voxels. Two 2D FLASH sequences were collected to estimate magnetic field maps and were used in post-processing to correct for geometric distortions. A high-resolution parallel imaging SPGR scan was acquired for anatomical localization (sagittal acquisition; TR=7.43 msec; TE=2.97 msec; TI=450 msec; NEX=1; flip angle=12°; FOV=250 mm; acquisition matrix=256 × 192; 172 slices; slice thickness=1 mm; resolution=0.98×0.98×1.0 mm).

2.5 FMRI and behavioral data analysis

2.5.1 FMRI preprocessing—Processing of the BOLD data incorporated a de-noising technique based on Independent Component Analysis (ICA) to remove structured physiological noise (Perlbarg, et al., 2007), eye motion artifact, and task-negative activation. The FMRI BOLD image sequences were reconstructed using AFNI (Cox & Hyde, 1997)[6] DICOM translation and corrected for geometric distortion with a customized script using the FSL (Smith, et al., 2004)[7] PRELUDE and FUGUE programs. The first four images in each run were deleted to eliminate T1 saturation effects. FSL tools were used for motion correction (midpoint acquisition as reference volume), slice timing correction, and spatial smoothing (5 mm FWHM Gaussian filter kernel). Each run was registered to the brain-

[6] http://afni.nimh.nih.gov
[7] http://www.fmrib.ox.ac.uk/fsl

extracted anatomy for that individual. The data sets were then submitted to single-session independent component analysis (ICA) using FSL MELODIC (Beckmann & Smith, 2004), with the number of output components automatically estimated. Briefly, the de-noising process assessed the relationship between the time series of the extracted independent components (ICs) and the BOLD signal from several regions of interest (ROIs) that capture known physiological distortion. ICs with significant association to the physiological noise estimates were removed from the data prior to analysis. Additionally, task-negative activity was removed. De-noising proceeded as follows. The ROIs were defined from each individual's anatomy and included the lateral and fourth ventricles (ventricle ROI), bilateral areas within both frontal and posterior white matter (white matter ROI), a region anterior to the superior aspects of the pons in the location of the basilar artery (Perlbarg, et al., 2007), and the eyes (Beauchamp, 2003; Haist, Adamo, Westerfield, Courchesne, & Townsend, 2005; Tregellas, Tanabe, Miller, & Freedman, 2002). The BOLD time series were extracted from the raw data for each of these ROIs and served as the dependent variables in separate stepwise multiple regression analyses using a forward selection criterion of $P < .01$ and backward removal criterion of $P < .05$ with the set of IC time series serving as the independent variables. These analyses were computed using SYSTAT (version 13; Chicago, IL). The stepwise regression results defined the subset of ICs that significantly predicted signal in each of the ROIs linked to physiological artifact. This subset of ICs formed the preliminary noise IC dataset. In another analysis, we calculated the Pearson correlation coefficient between each IC and a model of task-related (i.e., task-positive) activation generated by convolving the stimulus time series with a gamma function (Cohen, 1997). Individual ICs were removed from the preliminary noise subset if the IC had a task positive correlation of $r \geq .20$ ($P \leq .01$). Additionally, any IC, including ICs not previously identified as part of the noise subset, that was negatively correlated with task at $r \leq -.20$ ($P \leq .01$) was added to the noise subset. This procedure removed task-negative activation in the final BOLD data for a clearer exploration of task-positive activation. This final noise dataset of ICs was filtered from the subsequent reconstruction of each run and the resulting de-noised task runs were registered into standardized MNI space ("Colin 27"; Kochunov, et al., 2002) and resampled to 3 mm isotropic voxels. See Supplementary Information for findings about the improvement in FMRI BOLD signal achieved with this procedure relative to a traditional preprocessing method.

2.5.2 FMRI data scrubbing and inclusion criteria for individual participants—

The motion correction procedure generated measurements for the required rotation around the *x, y*, and *z* axes (i.e., *pitch, roll, and yaw*; measured in degrees) and translation in *x, y*, and *z* (measured in mm) for each volume to register to the standard image. Individual volumes were filtered from the analysis if rotation exceeded 1° or displacement exceeded 1 mm. This is a form of *scrubbing* procedure (Siegel, et al., 2013). In addition, as a second quality measure, we applied AFNI 3dToutcount to the motion corrected, slice time resampled, and spatially smoothed data to identify volumes that contained a large number of "outlier" voxels. A large number of outlier voxels may arise from a number of factors including residual uncorrected motion effects or scanner artifact. The program calculated the median absolute deviation (MAD) of the time series minus the linear trend. Outlier voxels were defined as those exceeding the range defined by the formula: $\alpha^* \sqrt{\frac{\pi}{2}} * MAD$, where α is the inverse of the reversed Gaussian continuous distribution function scaled by 0.001/N where N is the length of the time series (i.e., 168 volumes). Any volume that contained 10% or more outlier voxels was filtered from the analysis. Our inclusion criteria for individual participants required that less than 10% of the volumes (i.e., ≤ 17 volumes) were filtered in each of the four task runs; that is, exceeding this threshold in any single run eliminated a

participant from the study. The strict criteria assured that each participant contributed at least 90% of the available data from each of the four task runs.

2.5.3 FMRI analyses of individual participants—The FMRI data from individual participants were analyzed using a deconvolution multiple regression procedure (AFNI 3dDeconvolve). The hemodynamic response function (HRF) for each stimulus condition was modeled from a single-parameter block function (rectangular top hat filter applied to gamma variate function) convolved with the stimulus time series. The multiple regression model included the stimulus HRF parameters together with six parameters to account for motion artifacts (3 rotation and 3 displacement variables), and polynomial factors of no interest (i.e., linear, quadratic, and cubic functions). The resulting regression weights for faces, diverse objects, watches, and scrambled images were converted into percent signal values based on the voxelwise global mean activation estimated from the regression analysis.

2.5.4 Definition, measurement, and analysis of the fusiform face area (FFA)—The fusiform face area (FFA) was defined for each participant as an area or areas of the fusiform gyrus (primarily BA 37) bounded caudally by the posterior transverse collateral sulcus (including anterior BA 19 and posterior BA 37), rostrally by the anterior transverse collateral sulcus at the border with the parahippocampal gyrus (including posterior BA 20 and anterior BA 37), medially by the medial occipitotemporal sulcus, and laterally by the lateral occipitotemporal sulcus where face stimuli produced reliably greater activation than diverse objects at a voxelwise threshold of $P \leq .005$ with a minimum cluster volume of 64 μl. The cluster volume requirement assured that any activity defined as part of the FFA was at least the size of a single voxel in the "native space" resolution in which the data were acquired. All voxel clusters meeting these requirements were considered part the FFA even if clusters were not contiguous; that is, the FFA could include multiple active clusters within the fusiform gyrus and did not necessarily define a single area. We did not include the watch stimuli in the calculation of the FFA as this is not a commonly used stimulus in the field and most studies employ some form of diverse object category as the contrast to faces (c.f., Kanwisher & Yovel, 2006). The locations of the FFA region(s) from each participant were confirmed against their respective high-resolution anatomical scan to insure that voxels were restricted to the middle fusiform gyrus. Several measures of the FFA were calculated in each participant, including the total volume of the FFA (μl), the mean intensity across the ROI for each of the four stimuli (% signal), the mean face minus diverse object intensity across the ROI (% signal difference), and the location and intensity of the voxel showing the greatest face minus diverse object difference ("hot spot" location and % signal difference).

2.5.5 Group-level analyses of FFA—Developmental effects in past studies were investigated typically by using categorical bins across developmental stages. Unfortunately, the definition of age ranges for "children" and "adolescents" has been used inconsistently. Because our data were collected continuously across ages from children to adults, we evaluated developmental effects independent of age categories by using regression analyses with the natural logarithm of age for each participant regressed against the percent signal or FFA volume measures. When contrasting age-related effects, analysis of covariance (ANCOVA) was used that included age (natural logarithm transform) as the continuous between-subjects factor and task conditions as within subjects factors. This approach allows for the contrast of age-related regression slopes across task conditions (Thomas, et al., 2009).

The developmental trend in the spatial pattern of FFA ROIs was evaluated using a voxelwise binary logistic regression analysis (Neter, Kutner, Nachtsheim, & Wasserman, 1996). In each participant, every fusiform gyrus voxel was coded as either 1 or 0 depending

on whether it was classified as an FFA voxel or not, respectively. The logistic regression used this binary data to detect voxels that show a relationship to age and thus identified voxels within the FFA related to developmental trends. A cluster-threshold correction based on a Monte Carlo simulation was applied to the logistic regression results using a voxelwise threshold of $P \leq .05$ with a minimum cluster volume of 567 μl resulting in an effective $\alpha = .050$ (Forman, et al., 1995).

2.5.6 Group-level analyses of whole-brain activation—Developmental effects for whole-brain BOLD face preferential activation were evaluated using linear regression with the natural logarithm of age serving as the independent variable and the percent signal in each voxel with a positive value in the face versus diverse object contrast serving as the dependent variable. A cluster-threshold correction based on a Monte Carlo simulation was applied to these results using a voxelwise threshold of $P \leq .005$ with a minimum cluster volume of 297 μl resulting in an effective $\alpha = .050$.

2.5.7 Analysis of behavioral data—Accuracy, measured by d', and reaction time were analyzed using least squares linear regression against the natural logarithm of age.

2.5.8 Analysis of motion and scrubbing data—Rotation and translation motion data were analyzed using separate repeated measures ANOVAs with age group (fixed effect) and motion axis (fixed effect) as factors, with subject (random effect) nested within groups. Between groups post hoc analysis used the Least Significant Difference test. The number of filtered volumes data from the scrubbing procedure were analyzed using a one-way ANOVA with group as the factor. Possible associations between the number of filtered volumes and intensity and volume measures in the FFA were analyzed using Pearson correlation based on bootstrapping using 10,000 samples within each of the three groups separately.

3. Results

3.1 Behavioral Findings

Figure 2 shows the findings for accuracy and reaction time to respond to relatively rare gray backgrounds for each of the four stimulus categories, and includes the Pearson correlation coefficient for age against performance for each stimulus type. Technical difficulties during response collection precluded the analysis of data from one adult and two child participants, leaving an overall sample of 20 adults, 20 teens, and 28 children. A d' statistic was calculated to describe behavioral performance accuracy, as this measure considers both sensitivity and response bias. The association between age (natural logarithm) and the regression slopes for accuracy and reaction time across the four stimulus conditions were analyzed using separate analysis of covariance (ANCOVA) with stimulus condition as the within subjects factor and age as the continuous measure. There was a significant main effect of age for accuracy and reaction time indicating that accuracy increased and reaction time decreased with increasing age, accuracy: $F_{1,66} = 26.79$, $\eta_P^2 = .289$, $P < .001$, reaction time: $F_{1,66} = 32.65$, $\eta_P^2 = .331$, $P < .001$. The age × stimulus interaction was not significant in either contrast indicating that the regression slopes with respect to age did not differ between the stimulus types for accuracy or reaction time, accuracy: $F_{3,198} = 2.068$, $\eta_P^2 = .030$, $P = .106$, reaction time: $F_{3,198} < 1.00$, $\eta_P^2 = .006$, $P = .773$. Overall, accuracy performance was high across the age spectrum tested, demonstrating that all participants, including children, complied with the task instructions. Nevertheless, younger participants were less accurate and their responses were overall slower than older participants (e.g., teens and adults). An examination of the constituent aspects of the d' scores suggested that the

lower accuracy scores for younger participants was due to a positive response bias as indicated by higher false alarm rates.

3.2 Motion and Scrubbing Findings

Motion results for rotation and translation were analyzed in separate repeated measures ANCOVAs using the three axes of motion in each analysis as the within subjects factor and age (natural logarithm) as a continuous between-subjects factor. There was no interaction of age in either the rotation and translation analysis, rotation: $F_{1,69} < 1.00$, $\eta_P^2 = .001$, $P = .843$; translation: $F_{1,69} = 2.79$, $\eta_P^2 = .039$, $P = .100$. Therefore, our strict inclusion criteria and scrubbing procedure resulted in no statistically meaningful differences in motion across the age range of study participants. There was a significant negative correlation (Pearson Correlation Coefficient) between age (natural logarithm) and the number of filtered volumes from the FMRI time series indicating that younger participants had more filtered volumes than older participants, $r = -.330$, $R^2 = .109$, $P = .005$. However, the number of filtered volumes was not significantly correlated to either to the volume (cluster size) or intensity (percent BOLD signal) of activation within the right FFA that are described below, volume: $r = .005$, $R^2 < .001$, $P = .974$, intensity: $r = .132$, $R^2 < .017$, $P = .389$.

3.3 Fusiform Face Area (FFA) Findings

3.3.1 Observed FFA across participants—Right hemisphere FFA (rFFA) regions were detected in 16 of 21 adults (76.2%), 10 of 20 teens (50%), and 19 of 30 children (63.3%). The proportion of participants producing rFFA regions did not differ between groups, $\chi^2 = 3.03$, $P = .220$. Left hemisphere FFA (lFFA) regions were detected in 17 adults (81.0%), 10 teens (50%), and 23 children (76.7%). There was a trend for a difference in the proportion of participants producing lFFA regions due primarily to the lower proportion of teens producing lFFA ROIs relative to adults and children, $\chi^2 = 5.68$, $P = .058$. Table 2 shows descriptive statistics of the FFA ROIs. The location and total volume of activation in the ROIs is in accordance with many previous descriptions of the FFA (Berman, et al., 2010). Of note, we found reliable rFFA and lFFA ROIs in some of the youngest children that we evaluated, as young as 7 years, 4 months.

3.3.2 Volume of FFA Activation—Original: Mean volume findings from the rFFA and lFFA within groups are described in Table 2. Volume measures included all significantly activated clusters within the fusiform gyrus (see Sec. 2.5.4). Age-related effects were evaluated as a continuous measure with least squares linear regression using the volume data against the natural logarithm of age. These results are shown in Figure 3. Considering only participants that produced an FFA, the correlation between age and cluster size in the rFFA was significant and positive, $r_{43} = .258$, $R^2 = .066$, $P = .044$, but there was no significant relationship between age and lFFA cluster size, $r_{48} = -.081$, $R^2 = .006$, $P = .288$. Note that some prior developmental studies considered participants that did not show a reliable FFA as having a FFA cluster of size zero in statistical contrasts (Golarai, et al., 2007; Golarai, et al., 2010). Including participants that did not produce an FFA as zero cluster size also yielded a significant positive correlation between age and rFFA cluster size, $r_{69} = .234$, $R^2 = .055$, $P = .025$, but no significant relationship between age and lFFA cluster size, $r_{69} = -.036$, $R^2 = .001$, $P = .382$. To summarize, findings from this simple viewing task provided evidence for a significant, albeit modest increase in the size of the rFFA with development.

3.3.3 FFA Activation Intensity (% Signal)—The developmental trends for mean activation intensity within the rFFA and lFFA volumes against the natural logarithm of age are shown in Figure 4. Least squares linear regression showed no significant relationship between age and activation intensity in the rFFA, $r_{43} = -.06$, $R^2 = .003$, $P = .701$. In the lFFA, the relationship between age and activation intensity fell just short of significance

indicating that younger participants produced modestly greater activation than older participants, $r_{48} = -.27$, $R^2 = .074$, $P = .055$.

3.3.4 Location of FFA across development—We applied a voxelwise binary logistic regression analysis with the FFA ROIs from all the participants against the logarithm of age in order to characterize the spatial pattern for the FFA across development. This approach identified specific voxels in the FFA showing developmental trends. The results are shown in Figure 5. A region in the right hemisphere middle fusiform gyrus (Brodmann's area 37) showed a significant positive relationship with age; therefore, the voxels in this region showed an increased likelihood to be identified with the rFFA with increased age. The strongest relationship was found at Talairach coordinates $x = -38$ mm, $y = -44$ mm, $z = -16$ mm (Talairach & Tournoux, 1988). Equivalent MNI (SPM) coordinates computed using the GingerAle Convert Foci program (v. 2.1.1, http://www.brainmap.org/ale; Laird, et al., 2010; Lancaster, et al., 2007) were $x = -40$, $y = -47$, $z = -17$. No regions in the rFFA showed a negative relationship with age, and no voxels in the lFFA produced a significant positive or negative relationship. In summary, the area most consistently identified as FFA in adults across many face-processing studies using various face localizer tasks (Berman, et al., 2010) showed the greatest developmental effect in the fusiform gyrus.

3.3.5 Evaluation of FMRI preprocessing procedures on FFA findings—A novel feature of this study is the use of preprocessing procedures that removed physiological noise factors (*P*), eye motion (*E*), and most notably, task negative activity (*TNA*), a procedure we refer to as PETNA. To evaluate the potential effect the PETNA procedure had on measures of FFA across development relative to more traditional preprocessing methods, we compared the volume and intensity of activation observed in the rFFA following PETNA to a more typical preprocessing method that included motion correction, slice time resampling, spatial smoothing, and registration to standard MNI space. All of these procedures were also included in the PETNA processes (see Sec. 2.5.1 and Supplementary Information). Separate ANCOVAs for rFFA intensity and volume were conducted that used age (natural logarithm) as the continuous between-subjects variable and preprocessing procedures as the within-subjects factor. There was no significant main effect of preprocessing procedure in either analysis, rFFA volume: $F_{1,41} = 2.84$, $\eta_P^2 = .065$, $P = .100$, rFFA intensity: $F_{1,41} < 1.00$, $\eta_P^2 = .014$, $P = .457$, and no preprocessing procedure × age interaction, rFFA volume: $F_{1,41} < 1.00$, $\eta_P^2 = .001$, $P = .814$, rFFA intensity: $F_{1,41} = 1.19$, $\eta_P^2 = .028$, $P = .280$. Thus, the PETNA procedure had little impact on face preferential activation within the right fusiform gyrus relative to a more traditional preprocessing approach. This is consistent with the findings presented in the Supplementary Information Figure S1 showing no significant signal benefit in the fusiform gyrus region.

3.4 Whole-Brain Findings

3.4.1 Are-related changes in whole brain—Age effects across the whole brain for face-superior processing (i.e., faces versus diverse objects, the same contrast used to define the FFA) evaluated by linear regression are shown in the left panel of Figure 5 with a comprehensive description of regional activation provided in Table 3. No regions were observed that showed a positive relationship to age (i.e., older participants showing greater activation than younger participants). In contrast, multiple regions throughout the brain showed a negative relationship with age (i.e., activation reduced with age) including multiple regions in the extended face-processing system. These regions included bilateral inferior and middle temporal gyrus in the anterior temporal pole (BA 20 and 21, respectively), right hippocampus, bilateral amygdala, bilateral posterior cingulate (BA 31), left anterior cingulate (BA 32), right insula, and right inferior frontal gyrus (BA 45). Thus, in this simple viewing paradigm, age is negatively associated with activation of the extended

face-processing system and positively associated with activation within the right inferior occipital gyrus are commonly associated with the OFA, a component of the core face-processing system. Therefore, younger participants are showing hyperactivation of the extended face network relative to older participants (i.e., older adolescents and adult).

3.4.2 Evaluation of FMRI preprocessing procedures on whole brain activity patterns—The impact of the removal of physiological noise factors, eye motion artifact, and task-negative activity in preprocessing, i.e., the PETNA procedure, on the linear regression results for age (see Sec. 3.4.1) was contrasted with linear regression results using a traditional preprocessing regimen including motion correction, slice time correction, spatial smoothing, and MNI registration, together with the inclusion of motion parameters and polynomial factors of no interest in the multiple regression analysis. All of these processes were also included in the PETNA procedure. The results from the traditional preprocessing approach are shown in in the right panel of Figure 5. The traditional approach resulted in considerably fewer regions showing a developmental trend. However, a repeated measures ANCOVA using preprocessing procedure as the within subjects variable and age (natural logarithm) showed no regional activation differences between the two processing procedures. That is, in a direct comparison of the two approaches, no differences in age regression slopes were detected. This suggests that the improved statistical power of the PETNA procedure arose from an increase in the explained variance in the PETNA data and therefore a decrease in the observed standard error of the measurement relative to the traditional procedure. To evaluate this hypothesis, we calculated the mean BOLD activation (percent signal difference between faces and diverse objects) within a 6 mm radius “sphere” from one of the regions that showed a significant developmental trend in the PETNA analysis but not in the traditional preprocessing analysis, the region in the right hemisphere inferior frontal gyrus (ROI centered at Talairach coordinates $x = -46$ (right), $y = 32$ (anterior), $z = -4$ (inferior) (see Table 3). Within this region, the standard error of the measurement (SEM) of the regression slope for age in the PETNA data was 0.039, whereas the SEM of the age regression slope of the traditional data was 0.064. The difference in the SEM measures suggests approximately 190 participants would have been required to be tested using the traditional preprocessing approach to achieve the same statistical power obtained with the PETNA data in this right inferior frontal gyrus area. As further evidence, the partial η^2 value (η_P^2), a measure of effect size, was over 3.7 times greater in the PETNA linear regression for age compared to the traditional preprocessing approach (PETNA $\eta_P^2 = .119$ versus Traditional $\eta_P^2 = .032$). Thus, the PETNA procedure, and specifically the elimination of task-negative activity, substantially improved statistical power to detect age-related brain activation differences in this ROI and presumably throughout multiple brains areas that otherwise would have required an unreasonable number of participants to be tested under traditional preprocessing methods.

4. Discussion

4.1 Findings in context

The extensive neuroimaging study of mature visual face-processing abilities has produced a detailed description of regional brain areas preferentially sensitive to visual faces and face-related information, in addition to theories regarding the organization of these regions into functional systems in adults (c.f., Fairhall & Ishai, 2007; Haxby, et al., 2000). Our understanding of the developmental trajectory of brain regions involved in face processing is far less advanced. Many fundamental questions regarding the neural correlates of the development of face expertise remain open or incompletely addressed. Among these open questions are the following: 1) At what age do children reliably produce a functionally-defined fusiform face area? 2) Once the FFA emerges, how does it develop in terms of the

basic BOLD measures of intensity of activation and spatial extent of activation? 3) Does the FFA occupy the same region of the fusiform gyrus as that observed in adults, or is there a developmental trend toward the mature location in the lateral aspects of the middle fusiform gyrus? 4) Is there a developmental trajectory for the relationship of right and left FFA activation toward the mature pattern of a hemispheric bias toward the right hemisphere FFA? On a broader scale, almost nothing is understood about the development of face expertise outside the ventral occipital-temporal regions or "core face system" of the FFA, OFA, and superior temporal region. Thus, determining and characterizing the development of visual face expertise throughout the brain is a major foundational task for developmental cognitive neuroscience.

The present study attempted to address these fundamental questions with several novel approaches. First, in our study, we examined face-processing abilities in a relatively large sample of children between the ages of 6 and 12 years. In addition, we used a continuous sample of age from childhood through adolescence and into adulthood. The continuous measure of age allowed us to examine changes in face-related BOLD activation in finer age scale than the typical age groupings such as "children," "adolescents," and "adults." Second, we simplified our task demand to minimize extraneous cognitive processing factors that may complicate the analysis of visual face-processing abilities. Specifically, we used a simple viewing paradigm in which the behavior task assured that participants maintained attention during the task but did not require specific analysis or decisions about the stimuli themselves. Third, regarding fMRI data analysis, we used a novel FMRI preprocessing technique that removed task-negative activity from the raw FMRI data, along with artifacts from various physiological sources including eye movements (see Section 2.5.1). We have found that task-negative activity in children differs from adults both in distribution and intensity (Adamo, Han, & Haist, 2011). We showed that removing this confounding signal from FMRI data prior to analysis significantly improved the statistical power of whole brain analyses by substantially reducing error variance in the BOLD signal measures. Additional detailed information of the improvement in task signal is presented in the Supplementary Information. In the following discussion, we first address the fundamental questions related to the development of the FFA. Next, we summarize our findings regarding developmental patterns in whole-brain face-sensitive regions.

4.2 Fusiform Face Area Findings

The fusiform gyrus, and in particular the right hemisphere fusiform gyrus, is the most closely associated brain region for face-specific processing (Kanwisher & Yovel, 2006). Naturally, understanding the development of the FFA has been the central focus of most face-processing studies in children and adolescents.

In the present study, we defined FFA in individual participants using a standard formula of calculating voxels within the fusiform gyrus region that produced face activation that was significantly greater than activation to diverse objects. This could include a single cluster of activation, or multiple clusters distributed in fusiform gyrus. We found that the FFA can be reliably detected in the youngest children that we tested, specifically children as young as 7 years. One difficulty in determining whether other studies have produced similar results is that seldom are individual data provided about the FFA. In one study that did provide individual FFA descriptions across development, Peelen and colleagues (2009) showed that they also observed reliable FFA ROIs in children as young as 7 years using a sparse repetition one-back memory test contrasting faces to tools. In several other studies that reported only aggregate data, it seems reasonable to assume that right hemisphere FFAs (rFFA) were observed in children as young as 6 years. For example, Scherf et al. (2011) reported that they observed an rFFA in 11 of 13 participants in their age group spanning 6 to 10 years using a movie viewing task contrasting faces to places and scenes. Golarai et al.

(2007) found rFFA in 17 of 20 children between the ages of 7 and 11 years in a one-back memory task. Also, in a post-hoc analysis of their developmental data, Joseph et al. (2011) reported that they observed a reliable rFFA in 25% of children between the ages of 5 and 8 years in their simple viewing task that required a response to every picture stimulus. Overall, the preponderance of findings suggests that the rFFA can be reliably detected in young children, although right fusiform gyrus activation to faces is generally not found as consistently in children compared to adults (i.e., the proportion of children in a group producing a rFFA is typically lower than adults), and the volume and/or location often differs from the position of the rFFA in adults (Gathers, et al., 2004; Golarai, et al., 2007; Joseph, et al., 2011; Peelen, et al., 2009; Scherf, et al., 2007; Scherf, et al., 2011).

Given that the rFFA may be observed in young children, the obvious question is when does this region in the fusiform gyrus become mature in terms of standard FMRI metrics such as volume of activation and intensity of activation (i.e., percent signal). We found that the rFFA increased in volume with age ($r = .258$, $P = .087$). Joseph and colleagues (2011), using their simple viewing task did not find a significant difference in rFFA volume with age. Yet many other studies have reported a significant correlation between rFFA volume and age. The discrepancy between studies may be related to task differences; that is, some studies reporting a more dramatic volume change in rFFA across development employed tasks that placed greater cognitive demands on face-processing systems. For example, Golarai et al. (2007) used a one-back memory task and reported that adult rFFA volumes were 3.3 times larger on average than child rFFA volumes. Moreover, they found that rFFA volume correlated with recognition memory ability, suggesting that the task assessed memory factors over and above simple face-processing abilities. This finding was extended in a study examining FFA in adolescents (12 to 16 years) using a similar one-back memory task where adolescents produced significantly smaller rFFA volumes compared to adults, with a significant positive correlation found between age and rFFA volume (Golarai, et al., 2010). In agreement, Peelen et al. (2009), using their sparse repetition one-back task, also found a reliable correlation between rFFA volume and age. We intended our simple viewing task to minimize extraneous cognitive processing factors and equate performance across participants. However, we found significant age-related effects for both accuracy and reaction time indicating that younger participants did not perform as well as older participants, largely due to younger participants showing a greater tendency to produce "false positive" responses, or responding incorrectly to the non-target colored background. Thus, our task did not eliminate all cognitive factors differing with age, and produced FFA volume changes that appear consistent with other studies using what can be considered as simple viewing paradigms that have reported smaller rFFA volumes in children relative to adults and adolescents (Gathers, et al., 2004; Scherf, et al., 2007; Scherf, et al., 2011). Golarai et al. (2007) and Peelen et al. (2009) investigated cluster sizes for children and adults across various statistical thresholds and found that relative comparisons of rFFA volumes were consistent across thresholds ranging from quite liberal to very conservative; that is, findings from comparisons of rFFA volumes were robust and did not depend on the specific threshold selected. Taken together, the evidence appears to support the general conclusion that in simple viewing paradigms rFFA volume increases significantly with age. Nevertheless, it should be noted that the age-related effect in rFFA volume appears to be modest. We found that age accounted for only 6.6% of the total variance in rFFA volume, an estimate that is consistent with findings from Peelen et al. (2009). In summary, the preponderance of findings suggests that the rFFA increases in volume across development and does not reach maturity until mid-adolescence.

We found no developmental trend for a change in the intensity of rFFA activation measured by percent signal difference between faces and diverse objects. This finding is in agreement with Golarai et al. (2007), who found no differences in activation in the rFFA during their

one-back memory task between children, teens, and adults. In a study using three face-processing tasks including identity recognition, emotional expression recognition, and gaze determination, Cohen Kadosh and colleagues (2011) failed to find a significant effect of age in their right fusiform gyrus (rFG) ROI, although children produced numerically lower activation to faces relative to adults. However, Scherf and colleagues (2007; 2011) have reported reduced percent signal responses in children relative to adults from their passive viewing movie task. Peelen et al. (2009) compared statistical variables (i.e., *t* scores) across development as a measure of intensity of activation and reported significantly lower scores in children compared to adults. Statistical variables combine descriptions of mean activation with the measure of reliability and, as such, are not a direct intensity measure. In their report of the intensity of right fusiform face-preferential activity in the youngest children yet described, Cantlon and colleagues (2011) found similar activation intensity between children 4 to 5 years and adults using an event-related simple viewing paradigm (i.e., detect change in border color). The region they observed in the right fusiform gyrus for adults and children was substantially similar to a traditional rFFA region. Thus, at least in terms of intensity measures of face-superior activation in the rFFA, there is no consensus on evidence supporting an important association with development.

Some have argued that face preferential regions in the fusiform gyrus have reached full maturity by about 5 years and that the failure of many studies to detect the mature FFA in school-age children is due to technical shortcomings in FMRI acquisition methods based on the inappropriate use of adult-sized head coils in young children (McKone, Crookes, Jeffery, & Dilks, 2012). While technological advances such as using equivalently sized coils relative to the head size being imaged across the age range of development would almost certainly improve the ability to resolve functional activity with more precision, it is highly unlikely that the essential findings from the extant literature have significantly misjudged FFA development in children from 7 years and above. A careful review of the data from the use of custom-sized head coils suggest that while an increase in the signal-to-noise ratio (SNR) at the edge of cortex in 7-year-old children may see a 1.6-fold SNR improvement, as one moves into the interior of the brain, closer to the location of the fusiform gyrus, the improvement in SNR drops to a modest 5% (Keil, et al., 2011). Similarly, the SNR improvement in 4-year-old children at brain center is approximately only 9%. Note that the present study and another (Joseph, et al., 2011) found greater activation in children relative to adults in a region that is notoriously difficult to obtain FMRI signal (i.e., anterior temporal pole), and equivalent levels of activation are reported closer to the cortical surface (i.e., superior temporal sulcus/gyrus) where SNR problems with adult-size coils are reportedly greatest; thus one must argue that the fusiform gyrus is particularly or singularly vulnerable to SNR signal problems using adult head coils. Taken together with findings for a consistent level of percent signal in face versus non-face object contrasts across development in the fusiform gyrus, it would appear that a much more likely explanation for the variability in findings about the development of the FFA in children and adolescents is related to differences in methodology, such as the specific tasks used and analysis approaches that emphasize either group-level or individual-level calculation of the FFA.

The developmental change in the location of the FFA within the fusiform gyrus has been discussed in several studies qualitatively or using basic statistical tests between groups of the “hot spot” of FFA activation. Gathers et al. (2004) reported that the rFFA in children tended to be located in posterior fusiform gyrus (BA 19) whereas the adult rFFA fell in the typical middle fusiform gyrus (BA 37). Scherf and colleagues reported that the child rFFA tended to be located more posterior than adult and adolescent rFFA in one study (Scherf, et al., 2007), and medial in another (Scherf, et al., 2011). Cantlon and colleagues (2011) showed that the face-preferential regions in fusiform gyrus in children 4 to 5 years were very similar to that of adults. Here, we described the first formal statistical analysis for the developmental

change in FFA location. Logistic regression is a statistical method providing a means to conduct regression analyses using binary data together with continuous data. The results clearly demonstrated that the middle fusiform gyrus in the right hemisphere, the region most commonly associated with the FFA in adults (Berman, et al., 2010), is positively correlated with age. No age-related correlations were found in the left hemisphere fusiform gyrus, and importantly, no negative correlations with age were found in the right hemisphere fusiform gyrus. The latter finding appears to corroborate the somewhat inconsistent qualitative descriptions of the locations of child rFFA. That is, if children produce rFFAs that are inconsistently located within the fusiform gyrus, no region within the right fusiform gyrus should show a significant negative correlation. Of course, the failure to find regions with a negative relationship with age could result from various factors. For example, the immature fusiform gyrus region in children might allow for idiosyncratic locations in children that through experience and genetic influences become more regularized in the adult brain. On the other hand, such mapping trends might arise because there is less error in the fusiform gyrus region when registering adult brains to a standard brain compared to children. Further studies are needed to characterize these alternatives with reliability. Nonetheless, this finding is the first clear evidence for age-related changes in the spatial location of face-preferential processing regions in the fusiform gyrus.

4.3 Whole-Brain Findings: Core and Extended Face Networks

Studies evaluating developmental trends in face processing outside the fusiform gyrus have focused primarily on regions within the core face network, specifically the inferior occipital gyrus region referred to as the occipital face area (OFA), and superior temporal gyrus/sulcus (STG/STS) regions. For the right hemisphere OFA (rOFA), Joseph et al. (2011) reported increasing activation intensity with age. However, Scherf and colleagues (2007) found no reliable rOFA activation in their children between 6 and 10 years, but did observe a rOFA in the adolescents between 11 and 14 years, and both rOFA and lOFA in their adult group. Moreover, they found slightly lower face-preferential activation intensity ($P < .07$) for children relative to adults and adolescents within the adult-defined rOFA, with adults and adolescents producing similar activation intensity. They also noted that a lower proportion of children and adolescents produced a rOFA compared to an rFFA. Here, we did not define the rOFA as a specific ROI targeted for investigation. However, our task design allowed us to evaluate age as a continuous variable via regression analysis. We did not find an age-related association with activity in in the right inferior occipital gyrus region.

We found that viewing faces produced a negative association with age within the rSTG region. That is, children activated this core face network region more than adults. In contrast, Golarai and colleagues (2007) reported no developmental trend either in intensity or in volume of STS activation in their one-back memory task. Cohen Kadosh et al. (2011) also found no aging effect on face-preferential intensity across their identity matching, emotion matching, and gaze detection tasks, and likewise for Scherf and colleagues (2007) in their movie viewing task. However, the latter found a significant developmental trend in the size of rSTS with children producing smaller face-preferential regions relative to adolescents and adults. All of these findings appear to be challenged by Joseph et al. (2011) who reported reliable rSTS activation for adults but not for children or adolescents (see Table 3 Joseph, et al., 2011). However, no direct contrast between adults and the younger groups were reported so it is not possible to discern whether this apparent developmental effect is reliable. It is important to note that the studies that evaluated individual rSTS ROIs found that activation in the rSTS was less reliably detected in children than in adults relative to rFFA (Golarai, et al., 2007; Scherf, et al., 2007). This is one area where our linear regression approach using the full complement of participants might be superior to the standard ROI approach because of the increased statistical power afforded to the analysis

whereas subsamples of child and adolescent groups may provide biased estimates of rSTS activation.

Only one previous typical development FMRI study has considered activation throughout the brain including the regions of the extended face network (Joseph, et al., 2011), together with an additional report of functional connectivity using graph theory metrics including the same subjects from that study (Joseph, et al., 2012). They found regressive changes in BOLD activation, defined as greater activation in children than adults, in four extended face network regions, including the right temporal pole, opercular frontal gyrus, left angular gyrus, and middle temporal gyrus. Overall, they concluded that the pattern of changes they observed supported an Interactive Specialization (IS) model of development of face processing (Johnson, 2001, 2011). The IS model predicts some brain regions in the extended face system must show progressive changes due to increasing face specialization, whereas other regions must show regressive changes as these areas support cognitive functions linked to child face-processing abilities that are replaced by the mature brain systems supporting mature cognitive face-processing abilities.

A true developmental perspective requires the continuous measure of a phenomenon across the developmental range. Our study provides such a study of face processing from school-age children through adults with a whole-brain analysis of the extended face-processing network. We found extensive regional evidence for younger participants producing greater face preferential activation relative to older participants across extensive cortical and subcortical regions. These included many regions previously identified as part of the extended face network (Haxby, et al., 2000; Ishai, 2008; Ishai, et al., 2005), including the bilateral amygdala, bilateral anterior insula, bilateral hippocampus, bilateral anterior temporal pole, bilateral angular and supramarginal gyrus regions in the parietal lobe, left inferior frontal gyrus, and bilateral anterior cingulate cortex (see Table 3 & Fig. 5). These regions are typically activated in adults in a task-specific fashion. Also important to note, the hyperactivation of face-preferential regions was not simply related to a phenomenon in which children produced greater activation overall relative to adults; specifically, no such hyperactivation was observed in object-preferential processing areas. Thus, one defining characteristic of visual face-processing development is hyperactivation of the extended face network that develops to a focused use of regions depending on specific task requirements. We do not suggest, however, that all of the cortical and subcortical brain areas that produced hyperactivation in the faces versus objects contrast are necessarily part of the extended face network. Specifically, the behavioral results from our task suggest that our simple viewing paradigm may have tapped additional cognitive processing differences between younger participants and adults that may have influenced some regional activation differences, such as cognitive control (c.f., Somerville & Casey, 2010) and attention modulation (Konrad, et al., 2005). We view these results, as did Joseph et al. (2011), as consistent with the general framework of the IS model of development. The IS model predicts that all of the brain structures within a cognitive network, in this case the core and extended face networks, are at least somewhat active in the early stages of development, and the mature pattern of activation or correspondence of activation to task demands is shaped through a combination of experience and genetic factors (de Haan, Humphreys, & Johnson, 2002; Johnson, 2001, 2011). Here, we suggest the largely regressive nature of activation across the extended face networks is due to factors that shape and tune the selectivity of activation to fit particular task demands; in other words, experience provides the learning context for when to deploy a particular system to accomplish particular task demands. Our results show clearly that the developmental trajectory of the extended face system is prolonged and extends into mid-adolescence.

5. Conclusion

The present FMRI study of face processing used a continuous sampling of age across the developmental spectrum from middle childhood through adulthood and a whole-brain analysis to evaluate both the core and extended face networks. A simple viewing task was used in order to observe face-preferential processing with a minimal contribution of additional cognitive processing demands (e.g., memory). Within the right fusiform gyrus, there was a significant trend, albeit a modest one, for an increase in the volume of FFA with age, but no evidence for age-related effects in the intensity of activation in the rFFA. In the first formal test of location changes conducted across all three cardinal axes, a positive developmental trend demonstrated a gradual alteration of face-preferential processing to the classic area in the middle fusiform gyrus. Overall, certain aspects of the rFFA are stable from the earliest ages we tested (i.e., activation intensity); nonetheless the general conclusion, consistent with accumulating evidence from other developmental studies of face-preferential processing, is for a prolonged developmental trajectory within the right fusiform gyrus with maturity for face preferential processing not reached until middle adolescence. The provocative finding within the extended face network is that almost every key component of the network is hyperactivated in young children relative to adult activation, suggesting that mature patterns of task-specific engagement of regions to accomplish specific cognitive goals also has a prolonged developmental trajectory. One important question for future research is how these regions respond across development to tasks that tap specific cognitive processes.

Supplementary Material

Refer to Web version on PubMed Central for supplementary material.

Acknowledgments

We thank Janet Shin, Carolyn Sutter, Eunice Roh, Elizabeth Toomarian, Anna Hsu, and Belinda La for assistance in the conduct of this study and data analysis, Jerry Akshoomoff with assistance in manuscript preparation, Zachary Haist for assistance with statistical analyses, and Toby Thain for the Scramble Photoshop plugin. The National Institute of Child Health and Human Development Grants R01-HD060595, R01-HD041581, and R01-HD046526 supported this work.

Abbreviations

FFA	Fusiform Face Area(s)
OFA	Occipital Face Area
FG	fusiform gyrus
STS	superior temporal sulcus
VOT	ventral occipitotemporal cortex

References

Adamo M, Han J, Haist F. Denoising developmental FMRI data: Removal of structured noise from a passive-viewing task differentially impacts children and adults. Journal of Vision. 2011; 11:417–417.

Aristotle. Politics. The Internet Classics Archive. 350 B.C.E.

Avidan G, Behrmann M. Functional MRI reveals compromised neural integrity of the face processing network in congenital prosopagnosia. Current Biology. 2009; 19:1146–1150. [PubMed: 19481456]

Aylward EH, Park JE, Field KM, Parsons AC, Richards TL, Cramer SC, Meltzoff AN. Brain activation during face perception: evidence of a developmental change. Journal of Cognitive Neuroscience. 2005; 17:308–319. [PubMed: 15811242]

Beauchamp MS. Detection of eye movements from fMRI data. Magnetic Resonance in Medicine. 2003; 49:376–380. [PubMed: 12541259]

Beckmann CF, Smith SM. Probabilistic independent component analysis for functional magnetic resonance imaging. IEEE Transactions on Medical Imaging. 2004; 23:137–152. [PubMed: 14964560]

Behrmann M, Avidan G. Congenital prosopagnosia: face-blind from birth. Trends in cognitive sciences. 2005; 9:180–187. [PubMed: 15808500]

Berman MG, Park J, Gonzalez R, Polk TA, Gehrke A, Knaffla S, Jonides J. Evaluating functional localizers: The case of the FFA. Neuroimage. 2010; 50:56–71. [PubMed: 20025980]

Brambati SM, Benoit S, Monetta L, Belleville S, Joubert S. The role of the left anterior temporal lobe in the semantic processing of famous faces. Neuroimage. 2010; 53:674–681. [PubMed: 20600979]

Buckner RL, Andrews-Hanna JR, Schacter DL. The brain's default network: anatomy, function, and relevance to disease. Annals of the New York Academy of Sciences. 2008; 1124:1–38. [PubMed: 18400922]

Bushnell IW, Sai F, Mullin JT. Neonatal recognition of the mother's face. British Journal of Developmental Psychology. 1989; 7:3–15.

Bzdok D, Langner R, Hoffstaedter F, Turetsky BI, Zilles K, Eickhoff SB. The Modular Neuroarchitecture of Social Judgments on Faces. Cerebral Cortex. 2011

Cantlon JF, Pinel P, Dehaene S, Pelphrey KA. Cortical representations of symbols, objects, and faces are pruned back during early childhood. Cerebral Cortex. 2011; 21:191–199. [PubMed: 20457691]

Cassia VM, Turati C, Simion F. Can a nonspecific bias toward top-heavy patterns explain newborns' face preference? Psychological Science. 2004; 15:379–383. [PubMed: 15147490]

Cohen Kadosh K, Cohen Kadosh R, Dick F, Johnson MH. Developmental changes in effective connectivity in the emerging core face network. Cerebral Cortex. 2011; 21:1389–1394. [PubMed: 21045001]

Cohen Kadosh K, Henson RN, Cohen Kadosh R, Johnson MH, Dick F. Task-dependent activation of face-sensitive cortex: an fMRI adaptation study. Journal of Cognitive Neuroscience. 2010; 22:903–917. [PubMed: 19320549]

Cohen Kadosh, K.; Johnson, MH.; Dick, F.; Cohen Kadosh, R.; Blakemore, SJ. Cerebral Cortex. 2012. Effects of Age, Task Performance, and Structural Brain Development on Face Processing.

Cohen LB, Cashon CH. Do 7-month-old infants process independent features or facial configurations? Infant and Child Development. 2001; 10:83–92.

Cohen MS. Parametric analysis of fMRI data using linear systems methods. Neuroimage. 1997; 6:93–103. [PubMed: 9299383]

Cox RW, Hyde JS. Software tools for analysis and visualization of fMRI data. NMR in Biomedicine. 1997; 10:171–178. [PubMed: 9430344]

de Haan M, Humphreys K, Johnson MH. Developing a brain specialized for face perception: a converging methods approach. Developmental Psychobiology. 2002; 40:200–212. [PubMed: 11891633]

de Haan M, Pascalis O, Johnson MH. Specialization of neural mechanisms underlying face recognition in human infants. Journal of Cognitive Neuroscience. 2002; 14:199–209. [PubMed: 11970786]

Epstein RA, Higgins JS, Parker W, Aguirre GK, Cooperman S. Cortical correlates of face and scene inversion: a comparison. Neuropsychologia. 2006; 44:1145–1158. [PubMed: 16303149]

Fair DA, Cohen AL, Dosenbach NU, Church JA, Miezin FM, Barch DM, Raichle ME, Petersen SE, Schlaggar BL. The maturing architecture of the brain's default network. Proceedings of the National Academy of Sciences of the United States of America. 2008; 105:4028–4032. [PubMed: 18322013]

Fairhall SL, Ishai A. Effective connectivity within the distributed cortical network for face perception. Cerebral Cortex. 2007; 17:2400–2406. [PubMed: 17190969]

Forman SD, Cohen JD, Fitzgerald M, Eddy WF, Mintun MA, Noll DC. Improved assessment of significant activation in functional magnetic resonance imaging (fMRI): use of a cluster-size threshold. Magnetic Resonance in Medicine. 1995; 33:636–647. [PubMed: 7596267]

Freire A, Lee K. Face recognition in 4- to 7-year-olds: processing of configural, featural, and paraphernalia information. Journal of Experimental Child Psychology. 2001; 80:347–371. [PubMed: 11689035]

Friston KJ, Harrison L, Penny W. Dynamic causal modelling. Neuroimage. 2003; 19:1273–1302. [PubMed: 12948688]

Gathers AD, Bhatt R, Corbly CR, Farley AB, Joseph JE. Developmental shifts in cortical loci for face and object recognition. Neuroreport. 2004; 15:1549–1553. [PubMed: 15232281]

Gauthier I, Curby KM, Skudlarski P, Epstein RA. Individual differences in FFA activity suggest independent processing at different spatial scales. Cognitive, Affective & Behavioral Neuroscience. 2005; 5:222–234.

Gauthier I, Tarr MJ, Moylan J, Anderson AW, Skudlarski P, Gore JC. Does visual subordinate-level categorisation engage the functionally defined fusiform face area? Cognitive Neuropsychology. 2000; 17:143–164. [PubMed: 20945177]

Gobbini MI, Haxby JV. Neural systems for recognition of familiar faces. Neuropsychologia. 2007; 45:32–41. [PubMed: 16797608]

Golarai G, Ghahremani DG, Whitfield-Gabrieli S, Reiss A, Eberhardt JL, Gabrieli JD, Grill-Spector K. Differential development of high-level visual cortex correlates with category-specific recognition memory. Nature Neuroscience. 2007; 10:512–522.

Golarai G, Liberman A, Yoon JM, Grill-Spector K. Differential development of the ventral visual cortex extends through adolescence. Frontiers in Human Neuroscience. 2010; 3:80. [PubMed: 20204140]

Grill-Spector K, Knouf N, Kanwisher N. The fusiform face area subserves face perception, not generic within-category identification. Nature Neuroscience. 2004; 7:555–562.

Haist F, Adamo M, Westerfield M, Courchesne E, Townsend J. The functional neuroanatomy of spatial attention in autism spectrum disorder. Developmental Neuropsychology. 2005; 27:425–458. [PubMed: 15843105]

Haist F, Lee K, Stiles J. Individuating faces and common objects produces equal responses in putative face-processing areas in the ventral occipitotemporal cortex. Frontiers in Human Neuroscience. 2010; 4:181. [PubMed: 21206532]

Haxby JV, Gobbini MI, Furey ML, Ishai A, Schouten JL, Pietrini P. Distributed and overlapping representations of faces and objects in ventral temporal cortex. Science. 2001; 293:2425–2430. [PubMed: 11577229]

Haxby JV, Hoffman EA, Gobbini MI. The distributed human neural system for face perception. Trends in cognitive sciences. 2000; 4:223–233. [PubMed: 10827445]

Haxby JV, Hoffman EA, Gobbini MI. Human neural systems for face recognition and social communication. Biological Psychiatry. 2002; 51:59–67. [PubMed: 11801231]

Ishai A. Let's face it: it's a cortical network. Neuroimage. 2008; 40:415–419. [PubMed: 18063389]

Ishai A, Pessoa L, Bikle PC, Ungerleider LG. Repetition suppression of faces is modulated by emotion. Proceedings of the National Academy of Sciences of the United States of America. 2004; 101:9827–9832. [PubMed: 15210952]

Ishai A, Schmidt CF, Boesiger P. Face perception is mediated by a distributed cortical network. Brain Research Bulletin. 2005; 67:87–93. [PubMed: 16140166]

Johnson MH. Functional brain development in humans. Nature Reviews: Neuroscience. 2001; 2:475–483.

Johnson MH. Interactive specialization: a domain-general framework for human functional brain development? Developmental Cognitive Neuroscience. 2011; 1:7–21. [PubMed: 22436416]

Johnson, MH.; Morton, J. Biology and Cognitive Development: The Case of Face Recognition. Blackwell Oxford Uk & Cambridge Usa; 1991.

Joseph JE, Gathers AD, Bhatt RS. Progressive and regressive developmental changes in neural substrates for face processing: testing specific predictions of the Interactive Specialization account. Dev Sci. 2011; 14:227–241. [PubMed: 21399706]

Joseph JE, Swearingen JE, Clark JD, Benca CE, Collins HR, Corbly CR, Gathers AD, Bhatt RS. The changing landscape of functional brain networks for face processing in typical development. Neuroimage. 2012; 63:1223–1236. [PubMed: 22906788]

Kanwisher N, McDermott J, Chun MM. The fusiform face area: a module in human extrastriate cortex specialized for face perception. The Journal of Neuroscience. 1997; 17:4302–4311. [PubMed: 9151747]

Kanwisher N, Stanley D, Harris A. The fusiform face area is selective for faces not animals. Neuroreport. 1999; 10:183–187. [PubMed: 10094159]

Kanwisher N, Yovel G. The fusiform face area: a cortical region specialized for the perception of faces. Philosophical transactions of the Royal Society of London. Series B, Biological sciences. 2006; 361:2109–2128.

Kaplan JT, Freedman J, Iacoboni M. Us versus them: Political attitudes and party affiliation influence neural response to faces of presidential candidates. Neuropsychologia. 2007; 45:55–64. [PubMed: 16764897]

Keil B, Alagappan V, Mareyam A, McNab JA, Fujimoto K, Tountcheva V, Triantafyllou C, Dilks DD, Kanwisher N, Lin W, Grant PE, Wald LL. Size-optimized 32-channel brain arrays for 3 T pediatric imaging. Magnetic Resonance in Medicine. 2011; 66:1777–1787. [PubMed: 21656548]

Kelly DJ, Quinn PC, Slater AM, Lee K, Ge L, Pascalis O. The other-race effect develops during infancy: evidence of perceptual narrowing. Psychological Science. 2007; 18:1084–1089. [PubMed: 18031416]

Kelly DJ, Quinn PC, Slater AM, Lee K, Gibson A, Smith M, Ge L, Pascalis O. Three-month-olds, but not newborns, prefer own-race faces. Dev Sci. 2005; 8:F31–F36. [PubMed: 16246233]

Kochunov P, Lancaster J, Thompson P, Toga AW, Brewer P, Hardies J, Fox P. An optimized individual target brain in the Talairach coordinate system. Neuroimage. 2002; 17:922–927. [PubMed: 12377166]

Konrad K, Neufang S, Thiel CM, Specht K, Hanisch C, Fan J, Herpertz-Dahlmann B, Fink GR. Development of attentional networks: an fMRI study with children and adults. Neuroimage. 2005; 28:429–439. [PubMed: 16122945]

Kouider S, Eger E, Dolan R, Henson RN. Activity in face-responsive brain regions is modulated by invisible, attended faces: evidence from masked priming. Cerebral Cortex. 2009; 19:13–23. [PubMed: 18400791]

Kriegeskorte N, Formisano E, Sorger B, Goebel R. Individual faces elicit distinct response patterns in human anterior temporal cortex. Proceedings of the National Academy of Sciences of the United States of America. 2007; 104:20600–20605. [PubMed: 18077383]

Laird AR, Robinson JL, McMillan KM, Tordesillas-Gutierrez D, Moran ST, Gonzales SM, Ray KL, Franklin C, Glahn DC, Fox PT, Lancaster JL. Comparison of the disparity between Talairach and MNI coordinates in functional neuroimaging data: validation of the Lancaster transform. Neuroimage. 2010; 51:677–683. [PubMed: 20197097]

Lancaster JL, Tordesillas-Gutierrez D, Martinez M, Salinas F, Evans A, Zilles K, Mazziotta JC, Fox PT. Bias between MNI and Talairach coordinates analyzed using the ICBM-152 brain template. Hum Brain Mapp. 2007; 28:1194–1205. [PubMed: 17266101]

Langlois JH, Ritter JM, Roggman LA, Vaughn LS. Facial diversity and infant preferences for attractive faces. Developmental Psychology. 1991; 27:79–84.

Lee, K.; Quinn, PC.; Pascalis, O.; Slater, A. Development of Face-Processing Ability in Childhood. In: Zelaso, PD., editor. The Oxford Handbook of Developmental Psychology. Vol. Vol. 1. New York, NY: Oxford University Press; 2013. p. 338-370.Body and Mind

Leveroni CL, Seidenberg M, Mayer AR, Mead LA, Binder JR, Rao SM. Neural systems underlying the recognition of familiar and newly learned faces. Journal of Neuroscience. 2000; 20:878–886. [PubMed: 10632617]

Mazard A, Schiltz C, Rossion B. Recovery from adaptation to facial identity is larger for upright than inverted faces in the human occipito-temporal cortex. Neuropsychologia. 2006; 44:912–922. [PubMed: 16229867]

McKone E, Crookes K, Jeffery L, Dilks DD. A critical review of the development of face recognition: Experience is less important than previously believed. Cognitive Neuropsychology. 2012

Minear M, Park DC. A lifespan database of adult facial stimuli. Behavior Research Methods, Instruments, & Computers. 2004; 36:630–633.

Mondloch CJ, Le Grand R, Maurer D. Configural face processing develops more slowly than featural face processing. Perception. 2002; 31:553–566. [PubMed: 12044096]

Morris JP, Pelphrey KA, McCarthy G. Face processing without awareness in the right fusiform gyrus. Neuropsychologia. 2007; 45:3087–3091. [PubMed: 17643452]

Nestor A, Plaut DC, Behrmann M. Unraveling the distributed neural code of facial identity through spatiotemporal pattern analysis. Proceedings of the National Academy of Sciences of the United States of America. 2011; 108:9998–10003. [PubMed: 21628569]

Nestor A, Vettel JM, Tarr MJ. Task-specific codes for face recognition: how they shape the neural representation of features for detection and individuation. PloS One. 2008; 3:e3978. [PubMed: 19112516]

Neter, J.; Kutner, MH.; Nachtsheim, CJ.; Wasserman, W. Applied Linear Statistical Models. 4th ed.. Boston, MA: WCB McGraw-Hill; 1996.

Passarotti AM, Paul BM, Russiere JR, Buxton RB, Wong EC, Stiles J. The development of face and location processing: an fMRI study. Developmental Science. 2003; 6:100–117.

Passarotti AM, Smith J, DeLano M, Huang J. Developmental differences in the neural bases of the face inversion effect show progressive tuning of face-selective regions to the upright orientation. Neuroimage. 2007; 34:1708–1722. [PubMed: 17188904]

Peelen MV, Glaser B, Vuilleumier P, Eliez S. Differential development of selectivity for faces and bodies in the fusiform gyrus. Dev Sci. 2009; 12:F16–25. [PubMed: 19840035]

Pelphrey KA, Lopez J, Morris JP. Developmental continuity and change in responses to social and nonsocial categories in human extrastriate visual cortex. Frontiers in Human Neuroscience. 2009; 3:25. [PubMed: 19826492]

Perlbarg V, Bellec P, Anton JL, Pelegrini-Issac M, Doyon J, Benali H. CORSICA: correction of structured noise in fMRI by automatic identification of ICA components. Magnetic Resonance Imaging. 2007; 25:35–46. [PubMed: 17222713]

Phillips PJ, Moon H, Rizvi SA, Rauss PJ. The FERET evaluation methodology for face-recognition algorithms. IEEE Transactions on Pattern Analysis and Machine Intelligence. 2000; 22:1090–1104.

Phillips PJ, Wechsler H, Huang J, Rauss PJ. The FERET database and evaluation procedure for face-recognition algorithms. Image and Vision Computing. 1998; 16:295–306.

Pinsk MA, Arcaro M, Weiner KS, Kalkus JF, Inati SJ, Gross CG, Kastner S. Neural representations of faces and body parts in macaque and human cortex: a comparative FMRI study. J Neurophysiol. 2009; 101:2581–2600. [PubMed: 19225169]

Power JD, Barnes KA, Snyder AZ, Schlaggar BL, Petersen SE. Spurious but systematic correlations in functional connectivity MRI networks arise from subject motion. Neuroimage. 2012; 59:2142–2154. [PubMed: 22019881]

Quinn PC, Yahr J, Kuhn A, Slater AM, Pascalis O. Representation of the gender of human faces by infants: A preference for female. Perception. 2002; 31:1109–1121. [PubMed: 12375875]

Redcay E, Dodell-Feder D, Pearrow MJ, Mavros PL, Kleiner M, Gabrieli JD, Saxe R. Live face-to-face interaction during fMRI: a new tool for social cognitive neuroscience. Neuroimage. 2010; 50:1639–1647. [PubMed: 20096792]

Rhodes G, Byatt G, Michie PT, Puce A. Is the fusiform face area specialized for faces, individuation, or expert individuation? Journal of Cognitive Neuroscience. 2004; 16:189–203. [PubMed: 15068591]

Rolls ET. The representation of information about faces in the temporal and frontal lobes. Neuropsychologia. 2007; 45:124–143. [PubMed: 16797609]

Rossion B, Caldara R, Seghier M, Schuller AM, Lazeyras F, Mayer E. A network of occipito-temporal face-sensitive areas besides the right middle fusiform gyrus is necessary for normal face processing. Brain. 2003; 126:2381–2395. [PubMed: 12876150]

Scherf KS, Behrmann M, Humphreys K, Luna B. Visual category-selectivity for faces, places and objects emerges along different developmental trajectories. Dev Sci. 2007; 10:F15–F30. [PubMed: 17552930]

Scherf KS, Luna B, Avidan G, Behrmann M. "What" Precedes "Which": Developmental Neural Tuning in Face- and Place-Related Cortex. Cerebral Cortex. 2011; 21:1963–1980. [PubMed: 21257673]

Schulz KP, Clerkin SM, Halperin JM, Newcorn JH, Tang CY, Fan J. Dissociable neural effects of stimulus valence and preceding context during the inhibition of responses to emotional faces. Human Brain Mapping. 2009; 30:2821–2833. [PubMed: 19086020]

Siegel JS, Power JD, Dubis JW, Vogel AC, Church JA, Schlaggar BL, Petersen SE. Statistical improvements in functional magnetic resonance imaging analyses produced by censoring high-motion data points. Hum Brain Mapp. 2013 on line.

Slater A, Bremner G, Johnson SP, Sherwood P, Hayes R, Brown E. Newborn infants' preference for attractive faces: The role of internal and external facial features. Infancy. 2000a; 1:265–274.

Slater A, Quinn PC, Hayes R, Brown E. The role of facial orientation in newborn infants' preference for attractive faces. Developmental Science. 2000b; 3:181–185.

Smith SM, Jenkinson M, Woolrich MW, Beckmann CF, Behrens TE, Johansen-Berg H, Bannister PR, De Luca M, Drobnjak I, Flitney DE, Niazy RK, Saunders J, Vickers J, Zhang Y, De Stefano N, Brady JM, Matthews PM. Advances in functional and structural MR image analysis and implementation as FSL. Neuroimage. 2004; 23(Suppl 1):S208–S219. [PubMed: 15501092]

Somerville LH, Casey BJ. Developmental neurobiology of cognitive control and motivational systems. Curr Opin Neurobiol. 2010; 20:236–241. [PubMed: 20167473]

Spinoza, Bd. Ethics: Demonstrated in Geometric Order and Divided Into Five Parts. Middle Tennessee State University: MTSU Philosophy WebWorks; 1677. Part IV, Prop 35, Note

Stevens MC, Pearlson GD, Calhoun VD. Changes in the interaction of resting-state neural networks from adolescence to adulthood. Human Brain Mapping. 2009; 30:2356–2366. [PubMed: 19172655]

Supekar K, Uddin LQ, Prater K, Amin H, Greicius MD, Menon V. Development of functional and structural connectivity within the default mode network in young children. Neuroimage. 2010; 52:290–301. [PubMed: 20385244]

Talairach, J.; Tournoux, P. Co-planar Stereotaxic Atlas of the Human Brain. New York: Thieme Medical; 1988.

Taylor MJ, Batty M, Itier RJ. The faces of development: a review of early face processing over childhood. Journal of Cognitive Neuroscience. 2004; 16:1426–1442. [PubMed: 15509388]

Thomas MS, Annaz D, Ansari D, Scerif G, Jarrold C, Karmiloff-Smith A. Using developmental trajectories to understand developmental disorders. J Speech Lang Hear Res. 2009; 52:336–358. [PubMed: 19252129]

Tregellas JR, Tanabe JL, Miller DE, Freedman R. Monitoring eye movements during fMRI tasks with echo planar images. Human Brain Mapping. 2002; 17:237–243. [PubMed: 12395391]

Tsao DY, Livingstone MS. Mechanisms of face perception. Annual Review of Neuroscience. 2008; 31:411–437.

Turati C, Simion F, Milani I, Umiltà C. Newborns' preference for faces: What is crucial? Developmental Psychology. 2002; 38:875–882. [PubMed: 12428700]

Van Dijk KR, Sabuncu MR, Buckner RL. The influence of head motion on intrinsic functional connectivity MRI. Neuroimage. 2012; 59:431–438. [PubMed: 21810475]

Want SC, Pascalis O, Coleman M, Blades M. Recognizing people from the inner or outer parts of their faces: Developmental data concerning 'unfamiliar' faces. British Journal of Developmental Psychology. 2003; 21:125–135.

Wechsler, D. Wechsler Abbreviated Scale of Intelligence Manual. New York: The Psychological Corporation; 1999.

Weiner KS, Grill-Spector K. The improbable simplicity of the fusiform face area. Trends Cogn Sci. 2012; 16:251–254. [PubMed: 22481071]

Willenbockel V, Sadr J, Fiset D, Horne G, Gosselin Fdr, Tanaka J. The SHINE toolbox for controlling low-level image properties. Journal of Vision. 2010; 10:653.

Wojciulik E, Kanwisher N, Driver J. Covert visual attention modulates face-specific activity in the human fusiform gyrus: fMRI study. Journal of Neurophysiology. 1998; 79:1574–1578. [PubMed: 9497433]

Xu Y. Revisiting the role of the fusiform face area in visual expertise. Cerebral Cortex. 2005; 15:1234–1242. [PubMed: 15677350]

Yovel G, Kanwisher N. Face perception: domain specific, not process specific. Neuron. 2004; 44:889–898. [PubMed: 15572118]

Yovel G, Kanwisher N. The neural basis of the behavioral face-inversion effect. Current Biology. 2005; 15:2256–2262. [PubMed: 16360687]

Highlights

- We measured face-preferential activity in a continuous age sample from 6 years to adults.
- Fusiform face area (FFA) was found in children as young as 7 years.
- We found a modest increase in right FFA volume with age,and location of FFA changed with maturity.
- Children hyperactivated the entire “extended face network.”
- Face expertise development characterized by increasing modulation of face-preferred regions.

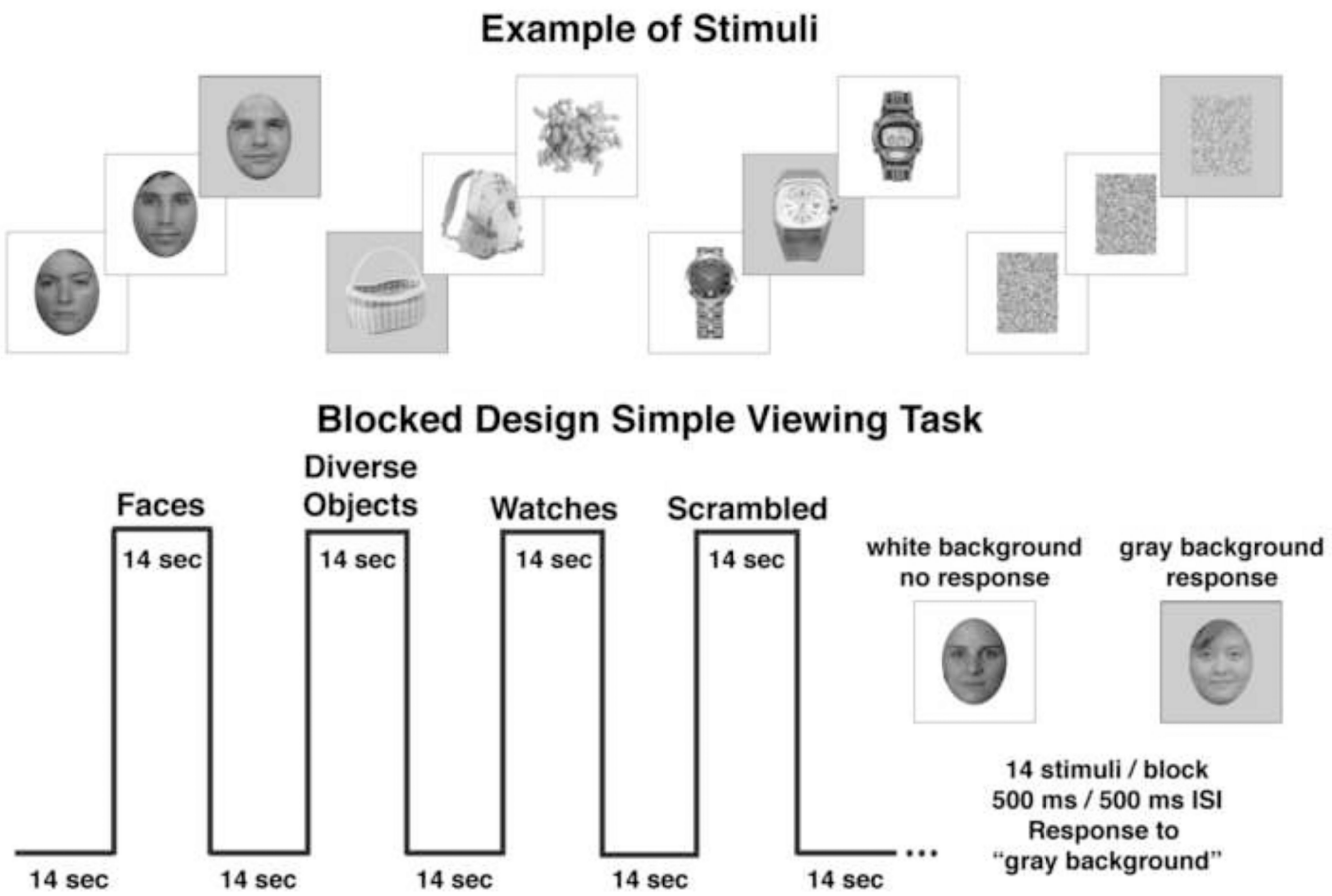

Figure 1.

Example of stimuli and design of the simple viewing task. All stimuli were presented in grayscale. All images were unique and not repeated during the test. Note that all watches were set to the same time. The order of stimulus task blocks was counterbalanced across the four task runs. The simple viewing task was equivalent to a traditional "face localizer task" typically used to functionally define the fusiform face area and other face preferential brain regions.

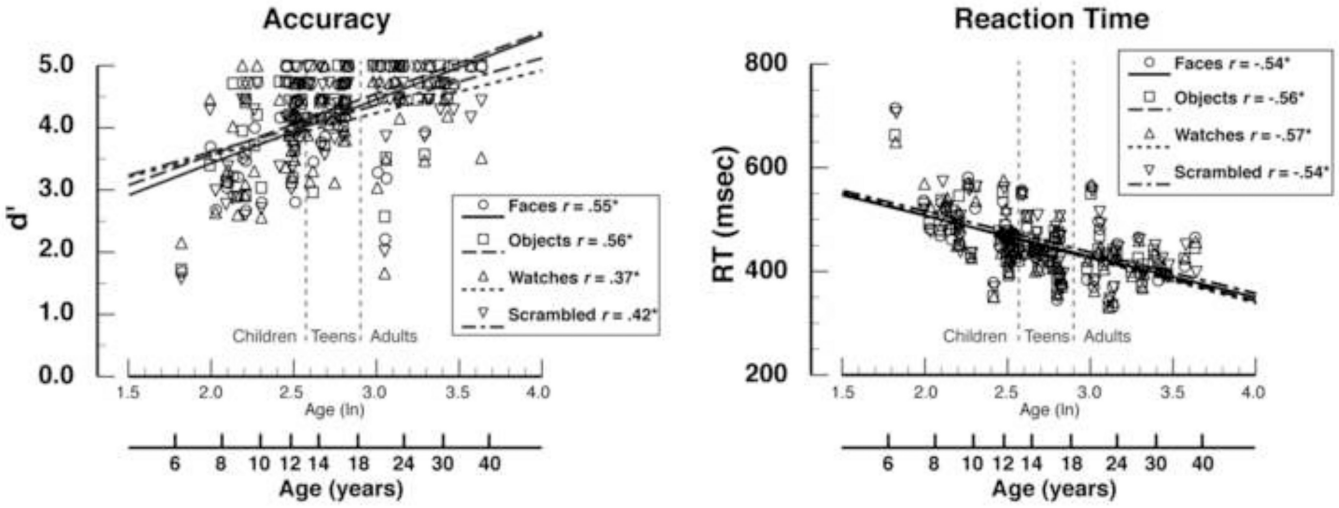

Figure 2.

Behavioral results for the four stimulus conditions from the simple viewing task. Accuracy (d') and reaction time results were analyzed as a continuous variable of age (ln = natural logarithm transformation). Linear regression lines and Pearson correlation coefficient (***r***) are provided. Separate ANCOVA analyses for accuracy and reaction time with age as a continuous between subjects variable showed reliable age effects for both measures, but no age × stimulus interactions; thus, younger participants were less accurate and slower to respond than older participants but there was no overall difference in responding to the four stimulus conditions. * = $P \leq .05$.

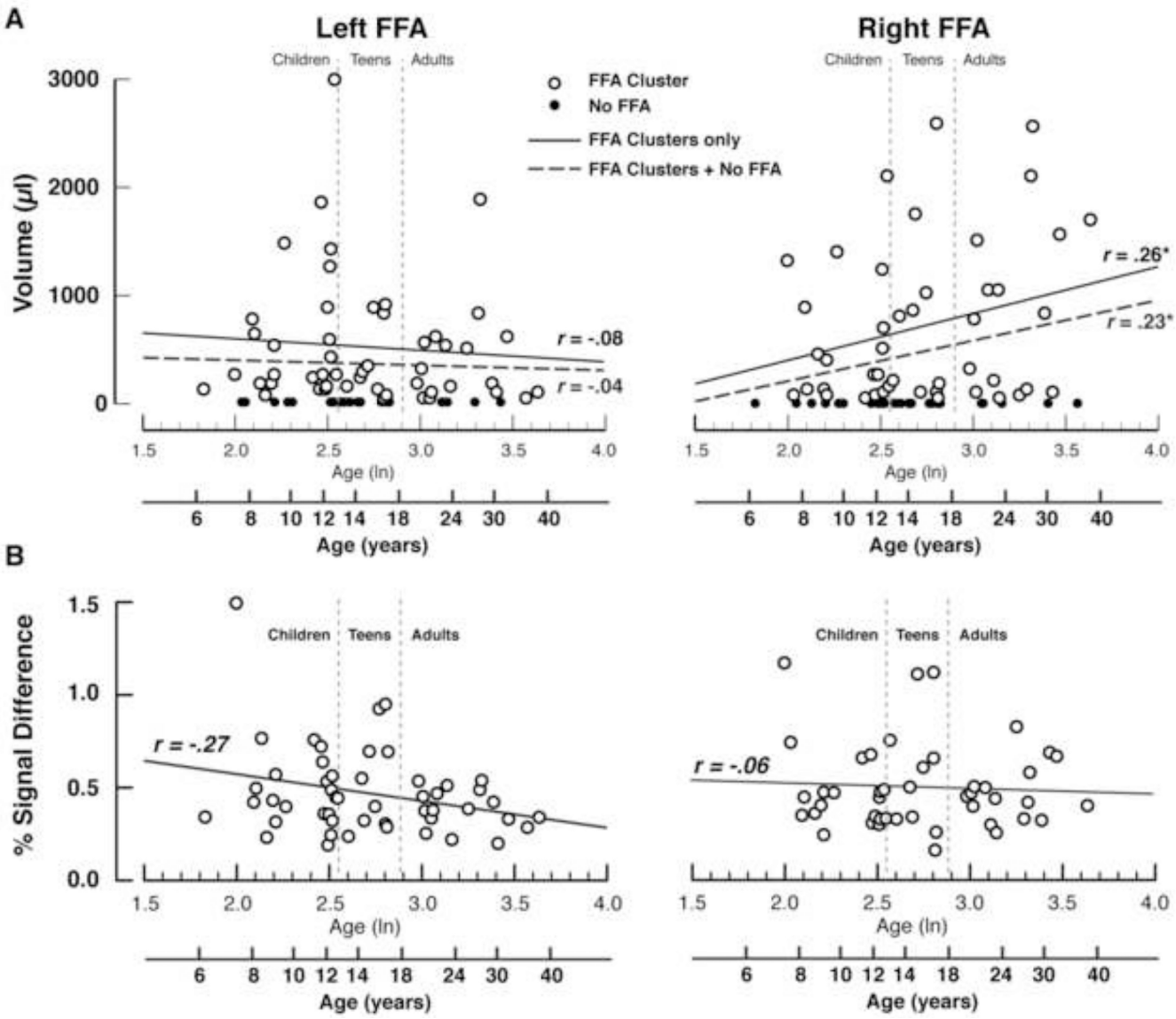

Figure 3.

Findings of FFA volume and intensity related to age. The FFA ROIs were defined by the contrast of faces versus diverse objects and included all clusters within the fusiform gyrus producing face > object activation. **A)** Left and right hemisphere FFA volume (1 μl = 1 mm^3) expressed as a continuous variable of age (ln = natural logarithm transformation). Linear regression lines and Pearson correlation coefficients (***r***, one-tailed) are provided. There was a significant positive correlation (solid line) with age in the volume of the right FFA using analysis that included only participants that produced a reliable FFA (open circles) and when participants that did not produce a reliable FFA (closed circles and dashed line) were included as a cluster size of zero. No significant age effect was observed in the left hemisphere. **B**) Mean percent BOLD signal within the left and right FFA ROIs expressed as a continuous variable of age for the faces versus diverse objects contrast Linear regression lines and Pearson correlation coefficients (***r***, two-tailed) are provided. Neither correlation was significant, although the left hemisphere FFA activation showed a trend toward a negative correction ($P = .055$).

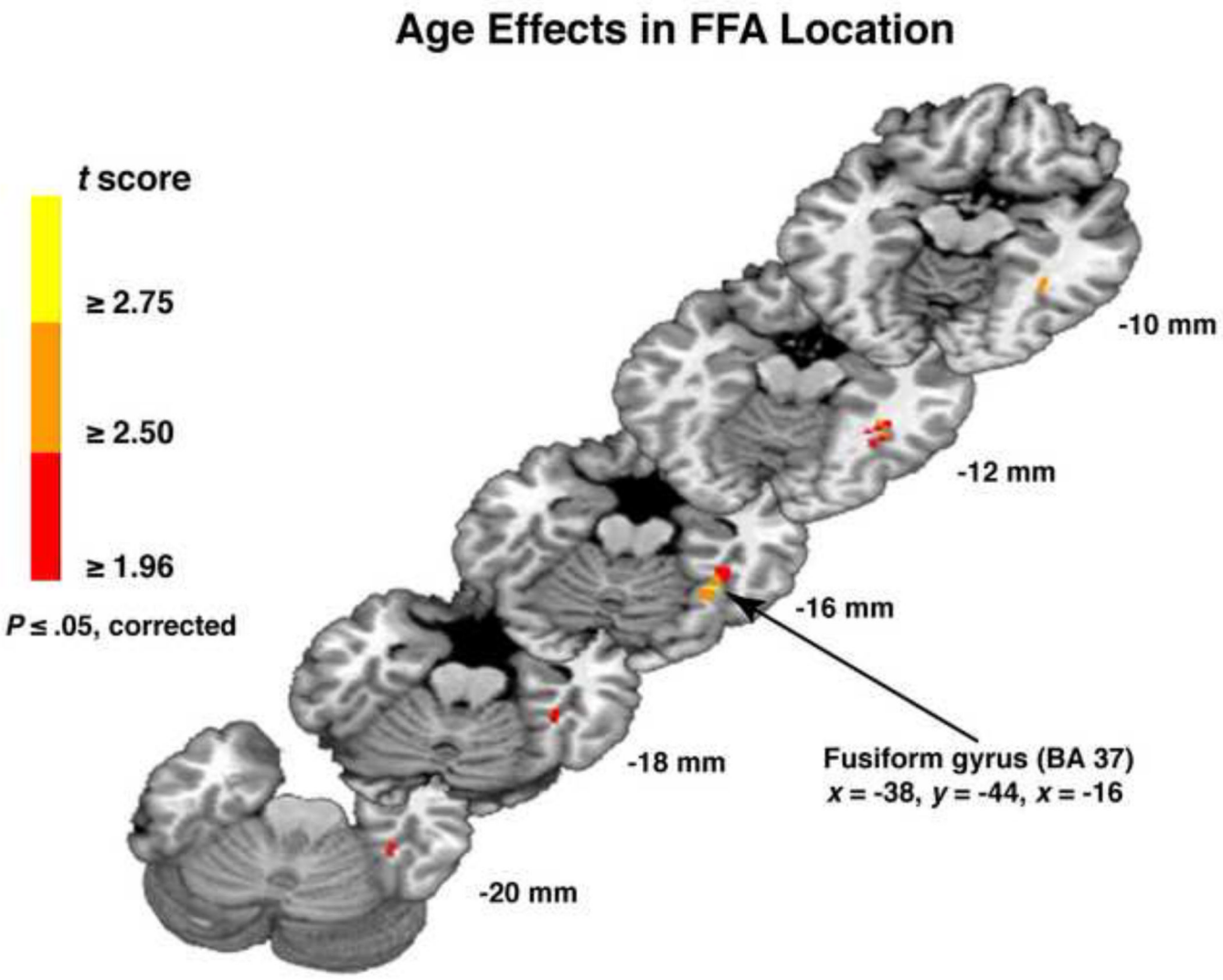

Figure 4.

Findings of FFA spatial differences related to age. The results of the logistic regression analysis that showed the spatial distribution of voxels within the fusiform gyrus (FFA) with a significant association to age. A cluster of voxels in the right fusiform gyrus (BA 37) showed a positive relationship indicating that this region is significantly more likely to be included in the FFA with increasing age of participants. The MNI (SPM) equivalent of the Talairach coordinates shown in the figure are $x = -40$, $y = -47$, $z = -17$. Color bar indicates the t score of the voxel in the logistic regression analysis.

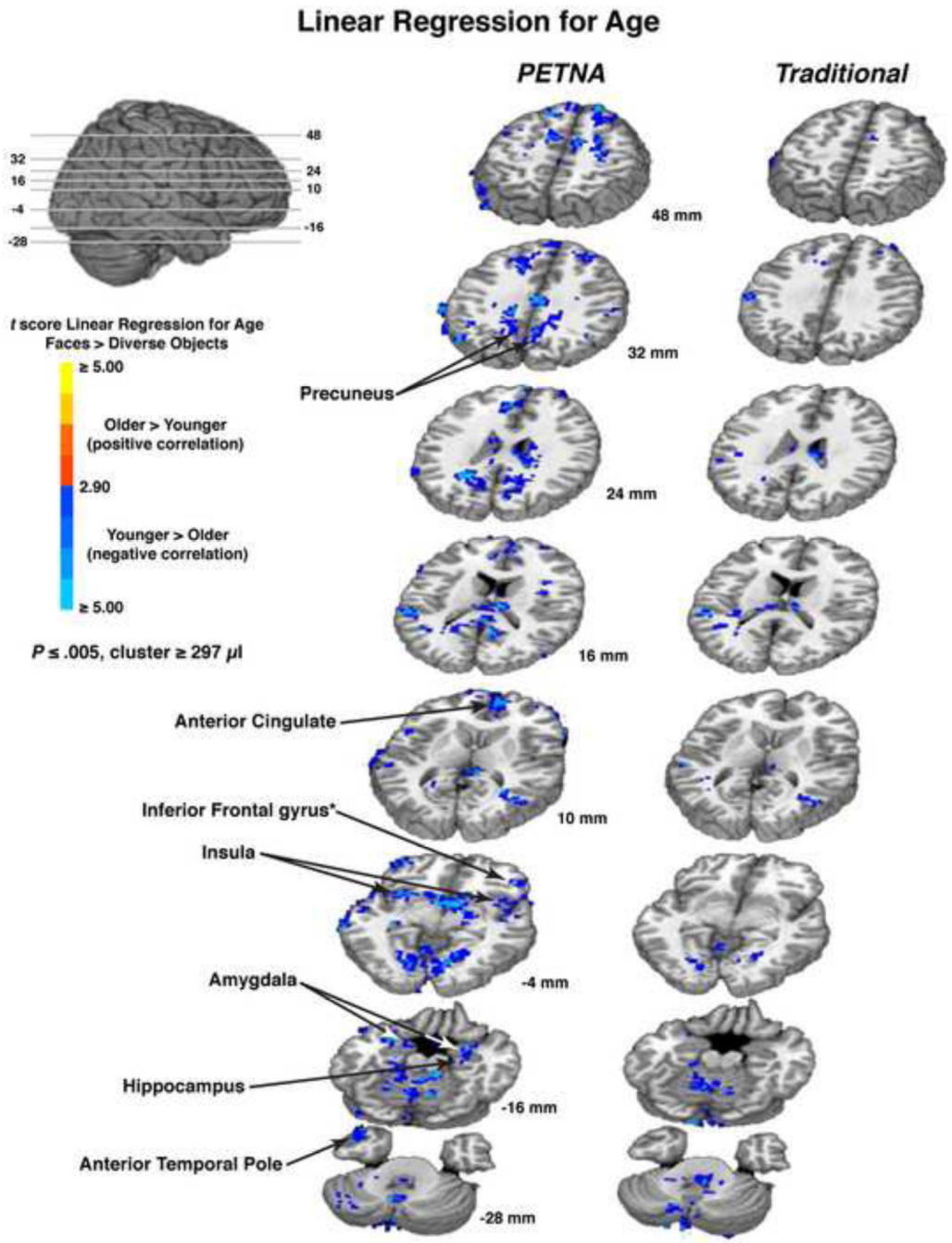

Figure 5.

Findings from the whole-brain analysis of regions showing face > diverse object activation with age considered as a continuous variable (natural logarithm of age transformation) using PETNA preprocessing methods (left panel) or traditional preprocessing measures (right panel). The PETNA data provided the main data for the study and the traditional data are shown as an illustration of the increased statistical power afforded by the removal of physiological noise factors (*P*), eye movement artifact (*E*), and task-negative activity (*TNA*). Using PETNA data, multiple regions showed a negative relationship to age, indicating that greater activation during the simple viewing task was observed in younger participants. Many of these regions are considered to be within the extended face-processing network

(highlighted). The color bar indicates the *t* score from the linear regression analysis with warm colors indicating a positive association with age and cool colors indicating a negative association with age. The levels of the slices presented are shown on the brain in the upper left corner. * = Right inferior frontal gyrus region examined in Results Section 3.4.2.

Table 1

Demographic information of study participants.

Group	N (F/M)	Age (Yrs-Mos)	WASI IQ Scores		
			FSIQ	VIQ	PIQ
All Participants					
Children	30 (15/15)	10−8	116.7	115.8	114.2
(*SD*)		*1–9*	*15.2*	*16.1*	*16.0*
Teens	20 (11/9)	15−9	116.1	117.6	111.2
(*SD*)		*1–10*	*10.7*	*12.4*	*10.3*
Adults	21 (9/12)	25−9	113.8	109.8	114.3
(*SD*)		*5–6*	*10.3*	*13.1*	*8.8*
Right FFA					
Children	19 (10/9)	10−5	116.6	114	115.8
(*SD*)		*2–3*	*17.2*	*17.0*	*16.6*
Teens	10 (6/4)	15−5	117.3	117.7	113
(*SD*)		*1–3*	*9.8*	*12.5*	*9.5*
Adults	16 (8/8)	25−6	113	109.5	113.5
(*SD*)		*5–4*	*9.18*	*12.4*	*8.3*
Left FFA					
Children	23 (12/11)	10−4	115.4	114.9	113.0
(*SD*)		2–3	15.1	15.7	16.1
Teens	10 (7/3)	15−6	118.2	117.5	115
(*SD*)		1–3	8.2	12.8	7.5
Adults	17 (8/9)	25−5	113.8	109.4	114.8
(*SD*)		6−3	10.9	14.2	8.3

Note: Data from participants in three analyses are shown. “All Participants” describes all eligible study participants that contributed to the whole-brain analyses. “Right FFA” and “Left FFA” describes the subsamples of participants that produced right and left FFA regions of interest, respectively. N (F/M) = number of participants and sex distribution in the sample. Age expressed in years-months. WASI = Wechsler Abbreviated Scales of Intelligence (Wechsler, 1999). FSIQ = Full Scale IQ; VIQ = Verbal IQ; PIQ = Performance IQ. IQ scores mean = 100, SD = 15. SD = standard deviation. Although data are presented in categorical age groups, all analyses of behavior and FMRI activation considered age as a continuous measure.

Table 2

Description of FFA regions of interest for children, teens, and adults.

FFA ROI	Total Volume* (μl)	Peak % Signal (F > O)	Talairach Coordinates of Peak % Signal Voxel			MNI Coordinates of Peak % Signal Voxel		
			x	*y*	*z*	*x*	*y*	*z*
Right Hemisphere								
Children (N=19)								
Mean	548.5	0.83	−39	−47	−17	−41	−50	−18
Median	270.0	0.62	−40	−46	−16	−42	−49	−17
SEM	134.1	0.15	1.4	2.2	1.0			
Teens (N=10)								
Mean	772.2	0.95	−43	−43	−19	−46	−46	−20
Median	513.0	1.03	−44	−42	−20	−47	−45	−22
SEM	266.7	0.15	1.0	3.4	1.2			
Adults (N=16)								
Mean	887.6	0.83	−41	−40	−18	−43	−43	−20
Median	810.0	0.81	−40	−38	−18	−42	−41	−20
SEM	201.8	0.10	1.1	2.5	1.0			
Left Hemisphere								
Children (N=23)								
Mean	664.4	0.79	39	−42	−18	43	−45	−20
Median	270.0	0.71	40	−40	−18	44	−43	−21
SEM	149.6	0.08	1.4	2.2	0.8			
Teens (N=10)								
Mean	396.9	0.71	40	−40	−18	44	−43	−21
Median	270.0	0.70	40	−39	−20	44	−42	−24
SEM	109.9	0.10	1.2	3.2	1.5			
Adults (N=17)								
Mean	408.2	0.57	40	−49	−16	44	−52	−18
Median	189.0	0.56	38	−46	−16	42	−49	−18
SEM	110.7	0.06	1.2	2.6	1.1			

Notes: Regions of interest were defined by contrast of faces versus diverse objects ($P \leq .005$). Volume = mean total volume of the fusiform gyrus showing face > object activity for those participants that produced an FFA (i.e., mean does not include zero values for participants that did not produce an FFA). Peak % Signal = percent signal difference at the voxel showing the greatest difference in the faces versus diverse objects contrast. Talairach coordinates follow the convention of the Talairach and Tournoux atlas (Talairach & Tournoux, 1988). Positive coordinate values indicate left (x), anterior (y), and superior (z). Coordinates are provided for the voxel showing the greatest intensity difference within the fusiform gyrus (i.e., "hot spot"). MNI (SPM) equivalent coordinates were calculated using the GingerALE Convert Foci program (v. 2.1.1, http://www.brainmap.org/ale; Laird, et al., 2010; Lancaster, et al., 2007). SEM = standard error of the mean.

Table 3

Whole brain face preferential regions (faces > diverse objects) showing significant linear response to age.

		Maximum Intensity Voxel in Region						
			Talairach Coordinates			MNI (SPM) Coordinates*		
Region	**BA**	t_{max}	*x*	*y*	*z*	*x*	*y*	*z*
Positive Relationship with Age								
None observed								
Negative Relationship to Age								
Occipital-Temporal								
R Lingual gyrus	19	3.90	−14	−70	−4	−14	−73	−2
R Middle temporal gyrus	37	3.87	−46	−64	12	−48	−66	−16
R Amygdala		4.14	−26	−2	−16	−27	−2	−22
R Hippocampus	28	3.24	−26	−16	−12	−27	−17	−16
L Lingual gyrus	18	3.78	14	−76	−6	16	−80	−4
L Superior temporal gyrus (ant. temporal pole)	38	3.65	44	16	−22	48	16	−32
L Middle occipital gyrus (ant. temporal pole)	38	3.45	40	14	−28	44	14	−38
L Amygdala		3.44	16	−4	−16	18	−4	−22
L Hippocampus	28	3.01	26	−22	−10	29	−23	−14
L Middle temporal gyrus	21	3.23	64	−26	−4	70	−26	−8
L Superior temporal gyrus	22	3.54	56	−10	0	62	−9	−5
Frontal								
R Ant. cingulate	32	4.02	−4	52	12	−3	58	3
R Insula (anterior)		3.89	−28	10	−4	−29	12	−10
R Inferior frontal gyrus	45	3.37	−46	32	−4	−49	35	−12
R Accumbens		3.34	−8	8	−6	−8	9	−12
R Superior frontal gyrus	8	3.16	−14	44	44	−14	53	40
R Superior frontal gyrus	9	3.70	−26	44	36	−27	52	31
R Caudate		3.09	−16	−10	24	−16	−7	23
R Precentral gyrus/Superior frontal gyrus	6	3.39	−22	−4	44	−22	2	45
R Cingulate gyrus	23/24	4.00	−4	−20	32	−3	−16	33
L Cingulate gyrus	24	3.38	4	−16	44	6	−11	46

		Maximum Intensity Voxel in Region						
			Talairach Coordinates			MNI (SPM) Coordinates*		
Region	**BA**	t_{max}	*x*	*y*	*z*	*x*	*y*	*z*
L Insula (posterior)		3.49	32	−20	2	36	−19	−1
L Superior frontal gyrus	21/22	3.78	58	−10	0	64	−9	−5
L Middle frontal gyrus	10	3.14	40	50	−4	44	54	−15
L Accumbens		2.95	4	8	−6	5	9	−12
L Precentral gyrus	4/6	3.27	34	−4	44	38	2	44
L Middle frontal gyrus	6	4.02	22	20	54	25	28	53
L Middle/Superior frontal gyrus	6/8	3.17	20	32	36	23	39	31
L Ant. cingulate	32/9	3.10	4	40	24	6	46	18
Parietal								
R Angular gyrus	39	3.03	−46	−50	26	−48	−49	30
R Supramarginal gyrus	40	3.34	−46	−28	26	−48	−26	28
R Post. cingulate	30/31	3.82	−10	−56	18	−9	−56	21
R Precuneus	18	3.29	−10	−56	24	−9	−56	28
R Precuneus	7	3.49	−8	−50	36	−7	−48	41
R Postcentral gyrus	3/5	3.04	−8	−44	66	−8	−52	73
L Precuneus	7	3.55	8	−50	36	10	−48	40
L Angular gyrus	39	3.62	44	−68	32	49	−67	37
L Supramarginal gyrus	40	4.16	62	−32	30	69	−29	31
L Cuneus	31	3.82	16	−52	24	19	−51	27
Subcortical/Other								
R Thalamus		3.75	−10	−22	18	−9	−20	18
L Cerebellum VII (Crus I)		4.47	28	−76	−24	31	−82	−24
L Cerebellum V/VI		3.73	26	−46	−22	29	−50	−25
Cerebellum Vermis VI		3.15	2	−58	−18	3	−62	−19

Notes: Region: R = right, L = left. BA = Brodmann's Area. Talairach coordinates follow the convention of the Talairach and Tournoux atlas (Talairach & Tournoux, 1988). Positive coordinate values indicate left (*x*), ant. (*y*), and Superior (*z*).

*MNI (SPM) equivalent coordinates were calculated using the GingerALE Convert Foci program (see Table 2 for details). t_{max} = *t* score for the beta coefficient from the linear regression analysis of activation (faces > diverse objects) against the natural logarithm of age at the maximum intensity voxel.